이학박사 학위논문

A Study on Modeling Glucose–Insulin Dynamics

글루코스–인슐린 역학에 관한 모델링연구

2013 년 8 월

서울대학교 대학원

수리과학부

조 용 진

A Study on Modeling Glucose–Insulin Dynamics

글루코스–인슐린 역학에 관한 모델링연구

지도교수 신 동 우

이 논문을 이학박사 학위논문으로 제출함

2013 년 4 월

서울대학교 대학원

수리과학부

조 용 진

조용진의 이학박사 학위논문을 인준함

2013 년 6 월

위 원 장	정 상 권	(인)
부위원장	신 동 우	(인)
위 원	전 영 목	(인)
위 원	박 춘 재	(인)
위 원	김 임 범	(인)

Abstract

A Study on Modeling Glucose–Insulin Dynamics

Yongjin Cho
Department of Mathematical Sciences
The Graduate School
Seoul National University

In this thesis, we analyze some mathematical models for glucose–insulin dynamics and estimate two key indices: insulin sensitivity (S_I) and glucose effectiveness (S_G). We address the advantages and disadvantages of each model from a mathematical perspective, and present an efficient estimation method for the relevant parameters and numerical algorithms to solve the glucose–insulin dynamics. A parameter sensitivity analysis is performed for each model, and numerical results are presented.

In addition, we propose a new model for glucose–insulin dynamics. Among many models, MINMOD Millennium has been widely used to estimate S_I in glucose–insulin dynamics. In order to explain the rheological behavior of glucose–insulin we attempt to modify MINMOD Millennium with fractional–order differentiation of order $\alpha \in (0, 1]$. We show that the new modified model has non–negative, bounded solutions and stable equilibrium points. Optimal fractional orders and parameters are estimated by using the nonlinear weighted least-squares method, the Levenberg–Marquardt algorithm, and the fractional Adams method for several subjects (normal subjects and type 2 diabetic patients). The numerical results confirm that S_I is significantly lower in diabetics

than in non–diabetics. Moreover, we find the new factor ($\tau^{1-\alpha}$) determining glucose tolerance and the relation between S_I and $\tau^{1-\alpha}$.

Keywords : glucose–insulin dynamics, insulin sensitivity, minimal model, fractional derivative

Student Number : 2010-30928

Contents

List of Figures

List of Tables

Chapter 1

Introduction

The pancreas plays a crucial role in regulating blood glucose–insulin concentration in the human body. In order to maintain the plasma glucose concentration within the normoglycemic range $(70-120 mg/dl)$, it provides glucagon released by α-cells or insulin secretion by β-cells in the so–called Langerhans islets [71]. When the blood glucose concentration level is high by food intake, glucose infusion, and so on, simultaneously, the β-cells release insulin. It produces the normal glucose concentration level by accelerating glucose disappearance into the periphery and liver and by inhibiting hepatic glucose production. Conversely, the blood glucose concentration level is low by exercises, fasting, and so on. At the same time, the α-cells release glucagon which results in increasing the blood glucose level by acting on liver cells and helping the liver cells to release glucose into the blood. Hence, the human body maintains the normal glucose concentration level. Figure 1.1 shows such glucose–insulin mechanism in human body.

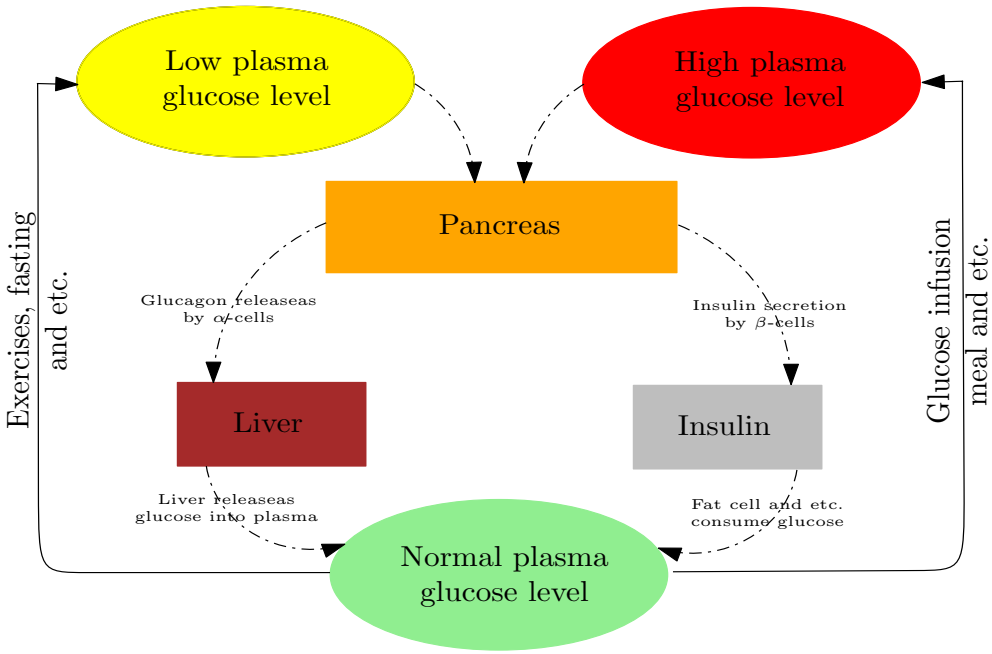

Figure 1.1: The glucose–insulin regulatory system.

Domineering or partial deficiency of insulin secretion by the pancreas, insufficiency of insulin's action in the glucose–insulin regulatory system, or both, lead to a metabolic disease known as diabetes mellitus [27, 30]. It is considered to have blood glucose problems known as hyperglycemia or hypoglycemia. Symptoms of principle hyperglycemia contain polyuria, polydipsia, weight loss, sometimes with polyphagia, and blurred vision. Chronic hyperglycemia may be accompany with increasing impairment to some infections. Life–threatening consequences of uncontrolled diabetes are hyperglycemia with ketoacidosis or the nonketotic hyperosmolar syndrome [30].

Long–term complications of diabetes include retinopathy with potential loss of vision; nephropathy leading to renal failure; peripheral neuropathy with risk of foot ulcers, amputations, and Charcot joints; and autonomic neuropathy causing gastrointestinal, genitourinary, and cardiovascular symptoms

and sexual dysfunction. Patients with diabetes have an increased incidence of atherosclerotic cardiovascular, peripheral arterial, and cerebrovascular disease. Hypertension and abnormalities of lipoprotein metabolism are often found in people with diabetes [30].

Diabetes is mainly classified into three categories.

Type 1 diabetes mellitus (formerly insulin dependent diabetes mellitus) is usually caused by a domineering deficiency in insulin secretion from autoimmune destruction of the pancreatic β-cells [30]. In order to regulate the blood glucose level, patients with type 1 diabetes need to be exogenous insulin therapy (admistering insulin or insulin pumps) [30].

Type 2 diabetes mellitus (formerly non–insulin dependent diabetes mellitus or adult–onset diabetes) is the much more widely form comparing to type 1 diabetes mellitus. Type 2 diabetes mellitus results from a combination of resistance to insulin action and an insufficient compensatory insulin secretion to response. Most patients with this type have obesity, and it result in some degree of insulin resistance [27, 30]. Patients with non–obese type 2 diabetes mellitus often reflect elevated circulating levels of free fatty acids (FFA) and triglycerides (TG) [30]. In contrast to type 1 diabetes mellitus, type 2 diabetes mellitus initially does not require insulin treatment to survive [30].

Gestational diabetes, the third main category, occurs when pregnant women without a previous diagnosis of diabetes develop a high blood glucose concentration level. Gestational diabetes mellitus (GDM) has similar symptoms with type 2 diabetes mellitus in some aspects, including a combination of relatively insufficient insulin secretion and responsiveness. Among all pregnant women, it occurs about 2%–5% and may develop or disappear after delivery. GDM is wholly treatable, but needs careful medication throughout the pregnancy. About 20%–50% of women with GDM proceed to type 2 diabetes mellitus

later in their life [102].

Diabetes mellitus is rapidly increasing prevalence in the world. In the United States, about 26 million Americans have diabetes, according to new estimates from the Centers for Disease Control and Prevention (CDC). In addition, 79 million U.S. adults were counted as prediabetes which has higher blood glucose concentration level than normal range, but not high enough to be diagnosed as diabetes [18]. In China, almost one in 10 adults have the disease while most cases remain undiagnosed [3]. In India, over 30 million have now been diagnosed with diabetes. The Crude prevalence rate in the urban areas of India is considered to be 9 percent. And the prevalence is about 3 percent of the total population in rural areas [29]. In addition, The International Diabetes Federation in October 2009 considered India to be the country with the most diabetic patients in the world [10]. The prevalence of diabetes for all age–groups worldwide was estimated to be 2.8% in 2000 and 4.4% in 2030. The total number of people with diabetes is predicted to rise from 171 million in 2000 to 366 million in 2030 [103].

Such significant diabetes meilltus is caused by the interaction of many factors (diet, weight, height, age, race, sex, exercise, family history, life style, the action of free fatty acid (FFA), and so on). Therefore, more research is still needed to see the mechanism of glucose–insulin.

The rest of this chapter is organized as follows. In Section 1.1, the history for modeling glucose–insulin dynamics is introduced briefly. In Section 1.2, the purposes of this dissertation are discussed.

1.1 A brief overview of the history for modeling glucose-insulin dynamics

Many mathematical models have been developed to understand the mechanism of glucose–insulin dynamics for diabetes mellitus. In general, mathematical models have been used to estimate the glucose disappearance and insulin sensitivity, which are used to study the relative dependency of glucose and insulin. Various models, from the simplest to the most comprehensive, have been proposed from as early as the 1960s [4–7, 12–14, 25, 28, 36, 43, 62, 69, 76, 79, 85, 86, 97, 98]. Among many valuable works, Toffolo *et al.* [98] proposed a simple minimal model by introducing a remote insulin compartment, and succeeded in explaining the delay action of glucose–insulin dynamics. Figure 1.2 shows the research situation for glucose–insulin dynamics with the minimal model.

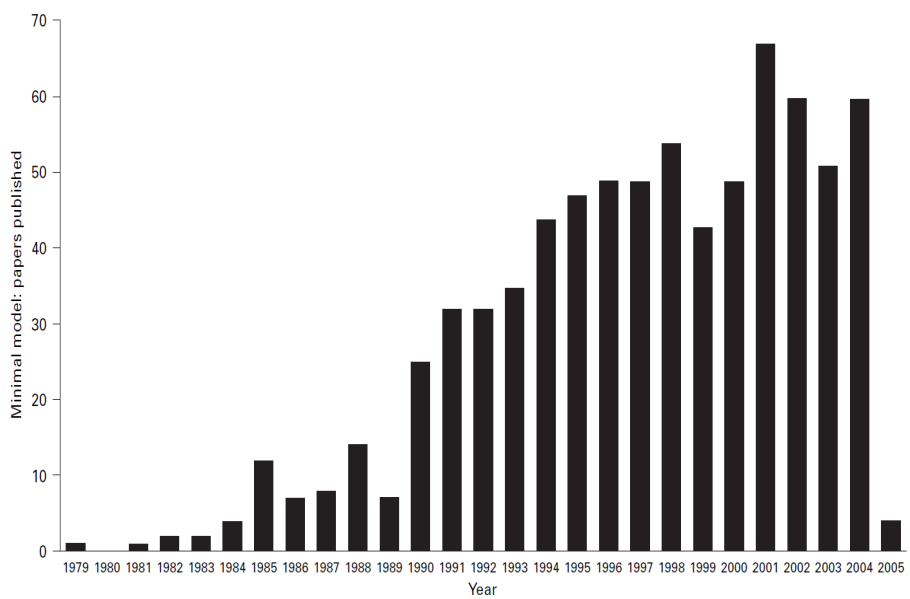

Figure 1.2: Studies using or studying the minimal model from 1979 to April 2005, estimated from the PubMed Citation Index [5].

In 1981, Bergman *et al.* [7] applied the minimal model to humans, and confirmed that it describes mathematically how glucose and insulin can control the production and disposal of glucose in the body. They also estimated two important indices: insulin sensitivity (S_I) and glucose effectiveness (S_G). Liver and peripheral tissues are mainly responsible for the disposition of administered glucose. The utilization process is controlled by insulin, enhancing glucose uptake. Simultaneously, an increase in glucose concentration augments the release of pancreatic insulin. Due to the existence of this feedback loop, in the minimal model, the system is decomposed into the effect of insulin to accelerate glucose uptake and the effect of glucose to enhance insulin secretion. The two subsystems have been described mathematically by the so–called glucose disappearance and insulin kinetics model. Pacini and Bergman [76] proposed a computer program called "MINMOD" based on this minimal model.

Since then, variant versions of MINMOD have been considered by numerous researchers [5, 12, 13, 25, 28, 43, 85, 86, 97]. Derouch and Boutayeb modified MINMOD to take account of parameters related to physical exercise [28].

Meanwhile, De Gaetano and Arino showed that MINMOD is structurally incorrect in a mathematical sense [25], and some of the results produced by MINMOD are not realistic because of the nonexistence of a positive equilibrium and the unboundedness of its solutions. To overcome some drawbacks inherited from MINMOD, they [25, 43] proposed an integro–delay–differential system and proved the positivity, boundedness, and stability of solutions using a square–wave delay integral kernel. Moreover, they offered a form of the dynamical system by coupling the two parts of MINMOD, and were able to describe the glucose–insulin system as a single–step parameter estimation process.

In 2003, Boston *et al.* [13] proposed the new glucose–insulin dynamics model (MINMOD Millennium), which is in some sense a contrast to the earlier versions of the minimal model. MINMOD Millennium provides estimates of insulin sensitivity and glucose effectiveness for almost every subject, solving the glucose disappearance model in such a way as to guarantee a non–negative solution.

For a better understanding of glucose–insulin dynamics, researchers have considered a number of parameters, such as diet, weight, height, age, race, sex, exercise, family history, and the action of FFA [36, 89].

Several researchers observed that the metabolism of FFA has a large impact on the glucose–insulin regulatory system [12, 15, 23, 48, 94–96]. Based on this, they tried to reflect the effect of FFA in their mathematical models [12, 79, 85, 86, 97]. In [92], Srinivasan *et al.* introduced a mathematical model for the control mechanism of FFA–glucose metabolism under resting conditions in normal humans. However, this model may have limited use in a research and clinical sense due to its many parameters and compartments. Thomaseth and Pavan [97] proposed a model based on the knowledge that suppression of lipolysis by insulin has a strong effect on intracellular and intravascular lipolysis. Their model predicts the FFA value using a remote insulin and measured plasma insulin value, but cannot describe the initial latency period in glucose–insulin dynamics [54]. Roy and Parker [85] developed a model of the relation between glucose–insulin and FFA, and observed an anti–lipolytic effect of insulin, a lipolytic effect of hyperglycemia, and an impairing effect of FFA on glucose uptake rate. They also estimated S_G, S_I, and pancreatic responsivity. Periwal *et al.* [79] examined a variety of mathematical models analogous to the minimal model of glucose disposal to quantify the combined influence on lipolysis and glucose disposal during the *insulin–modified frequently sampled*

intravenous glucose tolerance (IM–FSIGT) test.

Periwal *et al.* also presented a new model focusing on the effect of insulin on glucose disposal and lipolysis using IM–FSIGT. IM–FSIGT differs from the glucose–only FSIGT by the addition at 20 min of insulin in the form of either a bolus or a 5 min infusion [88]. Using Bayesian comparison methods, they confirmed that their model was the most balanced in comparison with others including Roy and Parker's and Thomaseth and Pavan's. In the following, we call Periwal's FFA model the lipolysis model. This section is based on [21].

1.2 Thesis overview

The aim of this thesis is to compare and analyze several glucose–insulin models, and to propose the new model based on those works.

In Chapter 2, we compare and analyze the mentioned models in Section 1.1, especially MINMOD Millennium and the lipolysis model. It is devoted to estimation parameters and performance a semi–relative sensitivity analysis [90], and we present numerical results for each model. We conclude this chapter with a discussion of our findings. This work is the improvement on [19]. And it will appear in [21].

In Chapter 3, we propose a system of fractional–order differential equations for modeling the glucose–insulin dynamics. In this chapter, we introduce a model that contains fractional–order differential equations of order $0 < \alpha \leq 1$ into MINMOD Millennium. It is devoted to the derivation and analysis of this fractional–order system in MINMOD Millennium. We describe the numerical method, including how to determine the optimal initial guess for the new model. The optimal fractional order and parameters are estimated for many experimental data (normal subjects and type 2 diabetic patients). From these results, we not only confirm that our analysis is correct, but also verify that the

insulin sensitivity (S_I) in diabetics is significantly lower than in non–diabetics. Moreover, we find the new factor ($\tau^{1-\alpha}$) determining glucose tolerance and the relation between S_I and $\tau^{1-\alpha}$. This work is from a paper in preparation with Imbunm Kim and Dongwoo sheen [20].

Chapter 2

Models and their analysis

2.1 Models and their analysis

In this section, we are interested in analyzing mathematical models that explain the metabolism of the glucose–insulin system using the *frequently sampled intravenous glucose tolerance* (FSIGT) test. In the standard FSIGT, a bolus of glucose (300 mg/kg) is intravenously injected, and blood samples are collected over a 3 hour period following the injection.

2.1.1 MINMOD

In 1986, Pacini and Bergman [76] introduced MINMOD to explain the dynamics of glucose–insulin. In this model, they considered MINMOD as a glucose disappearance model, and used it to calculate insulin sensitivity and glucose effectiveness from FSIGT. Plasma insulin $I(t)$ enters the "remote compartment $X(t)$," where it is active in accelerating glucose disappearance into the periphery and liver, and in inhibiting hepatic glucose production. Explicit

definitions of $X(t)$ and other parameters in terms of fractional turnover constants are found in [6]. Pacini and Bergman also considered MINMOD as an insulin kinetics model for calculating pancreatic responsivity.

This process can be described by the following system of ordinary differential equations.

$$\frac{dG(t)}{dt} = -(S_G + X(t))G(t) + S_G G_b,\ G(0) = G_0, \tag{2.1a}$$

$$\frac{dX(t)}{dt} = -p_2(X(t) - S_I(I(t) - I_b)),\ X(0) = 0, \tag{2.1b}$$

$$\frac{dI(t)}{dt} = \gamma(G(t) - h)t - nI(t),\ I(0) = I_0, \tag{2.1c}$$

where

- $G(t)$ $[mg/dl]$ is the plasma glucose concentration at time t $[min]$;
- $X(t)$ $[min^{-1}]$ is the insulin action in proportion to interstitial insulin;
- $I(t)$ $[\mu U/ml]$ is the plasma insulin concentration at time t $[min]$;
- G_b $[mg/dl]$, I_b $[\mu U/ml]$ are the basal glucose and insulin values, respectively;
- S_G $[min^{-1}]$ is the glucose effectiveness, which is the ability of glucose *per se* to enhance its own disappearance at the basal insulin level;
- p_2 $[min^{-1}]$ is a parameter describing the removal rate of insulin from the interstitial space;
- S_I $[min^{-1}(\mu U/ml)^{-1}]$ is the insulin sensitivity, which is the quantitative influence of insulin to increase the enhancement of glucose of its own disappearance in the steady state;
- n $[min^{-1}]$ is the first–order decay rate constant for insulin;

- γ $[(\mu U/ml)(mg/dl)^{-1}min^{-2}]$ is the rate of pancreatic release of insulin;
- h $[mg/dl]$ is the pancreatic target glycemia;
- G_0 $[mg/dl]$, I_0 $[\mu U/ml]$ are the initial plasma glucose and insulin concentrations, respectively.

This model describes the glucose–insulin dynamics with the eight parameters S_G, p_2, S_I, n, γ, h, G_0, and I_0. The parameters n and γ are related to pancreatic responsivity. $\dfrac{I_{max} - I_b}{n(G_0 - G_b)}$ means the first pancreatic responsivity, which is represented as a bolus of insulin entering the plasma compartment at the time of the glucose injection, where I_{max} is the computed maximum of the first peak insulin release. $\gamma \cdot 10^4$ is the second pancreatic responsivity, the rate of increase of the second–phase secretion in proportion (by γ) to the degree by which glucose exceeds a threshold level (h) [6].

Despite its simplicity, MINMOD provides a good description of the composite effects of insulin secretion and insulin sensitivity on glucose tolerance and the risk for diabetes [7, 76]. However, this model does not guarantee the positivity of solutions. $X(t)$ and $I(t)$ may become negative as time goes on. Also, the model is sensitive to the initial values of parameters, especially the initial condition (G_0, I_0). In order to overcome such difficulties, De Gaetano and Arino [25] have modified equation (2.1c) by introducing the positive threshold function $(G(t) - h)^+$ and shifting I_0 to $I_0 + I_b$. As a result, $X(t)$ and $I(t)$ have non–negative values for all time values [25]. In addition, they [25] proved the useful following statements :

1. Suppose $G_b > h$ and $\limsup_{t\to\infty} G(t) > h$. Then $\limsup_{t\to\infty} X(t) = \infty$,
2. Suppose $\limsup_{t\to\infty} G(t) < h$, then $G_b \leq h$,
3. For any value $h < G_b$, the system does not admit an equilibrium.

4. If the subject is considered to be at steady state before the glucose bolus, then G_b must be lesser than or equal to h.

5. Let $S_I > 0,\ h = G_b,\ G_0 > G_b$. Assume $G(t)$ and $X(t)$ bounded. Then there exists $T > 0$ such that $G(t) > G_b$ for all $t < T$, $G(T) = G_b$, and $G(t) < G_b$ for all $t > T$.

2.1.2 MINMOD Millennium

MINMOD Millennium is a computer program for the estimation of glucose effectiveness and insulin sensitivity from FSIGT. MINMOD Millennium only considers the glucose disappearance model with given insulin data. This process can be described by the following system of ordinary differential equations.

$$\frac{dG(t)}{dt} = -(S_G + X(t))G(t) + S_G G_b, \quad G(0) = G_0, \tag{2.2a}$$

$$\frac{dX(t)}{dt} = -p_2(X(t) - S_I(I(t) - I_b)^+), \quad X(0) = 0, \tag{2.2b}$$

$$(I(t) - I_b)^+ = \begin{cases} I(t) - I_b & I(t) \geq I_b, \\ 0 & I(t) < I_b, \end{cases} \tag{2.2c}$$

where $I(t)$ is an input variable and $G(t)$, $X(t)$ are output variables. And we consider $I(t)$ to be bounded and piecewise C^1 function.

Before studying the stability of the equilibrium solution, we will discuss the positivity and boundedness of solutions to system (2.2).

Proposition 2.1.1. *Let $G(t)$ and $X(t)$ satisfy (2.2). Then, $G(t)$ and $X(t)$ are positive for all $t > 0$. Moreover, we have*

$$G(t) = \frac{1}{\mu(t)} \left(G_0 + S_G G_b \int_0^t \mu(u)\, du \right) \quad \forall t \geq 0, \tag{2.3}$$

where $\mu(t) = e^{\int_0^t (S_G + X(u))\, du}$ *and*

$$G(t) \le G_b + (G_0 - G_b)e^{-S_G t} \quad \forall t > 0. \tag{2.4}$$

In particular,

$$\limsup_{t\to\infty} \; G(t) \le G_b. \tag{2.5}$$

Proof. By a direct calculation of (2.2b), we obtain

$$X(t) = p_2 S_I \int_0^t e^{-p_2(t-u)} (I(u) - I_b)^+ du.$$

Thus, it follows that $X(t) \ge 0$ for all t.

To prove (2.3), let $\mu(t) = e^{\int_0^t (S_G + X(u))\, du} (> 0)$. Then, (2.2a) gives

$$\int_0^t \frac{d}{ds} \left(\mu(s) G(s)\right) ds = \int_0^t S_G G_b \mu(s) ds,$$

and we obtain (2.3). The positivity of $G(t)$ is also checked for all $t > 0$ from its explicit form (2.3). From (2.2a), we have

$$\frac{dG}{dt}(t) \le -S_G G(t) + S_G G_b.$$

Let $L(t) = G(t) - G_b$. Then, the above inequality can be rewritten as follows:

$$\frac{dL}{dt} + S_G L \le 0,$$

which leads to

$$L(t) \le L(0) e^{-S_G t} \quad \forall t > 0.$$

Therefore, we have (2.4) and (2.5). This completes the proof. □

In order to understand the steady–state properties of this system, consider the steady state for $I(t)$. Using actual experimental results [7, 8, 25, 50, 66, 77, 79, 84, 99], I can see that $I(t)$ reaches the steady state (I_∞), which is in the neighborhood of I_b, due to the homeostasis of insulin. By recalling Definition 2.1.2 to Theorem 2.1.6 (See the pages 135–136 and 217–222 in [51]), we introduce the concept of input–to–state stability. Let us denote by $||\cdot||$, the l_2 norm.

Consider the system of ODEs

$$\dot{\mathbf{x}} = \mathbf{f}(t, \mathbf{x}, \mathbf{u}), \tag{2.6}$$

where $\mathbf{f} : [0, \infty) \times D \times D_u \to \mathbb{R}^n$ is piecewise continuous in t and locally Lipschitz in $\mathbf{x}$ and $\mathbf{u}$, $D \subset \mathbb{R}^n$ is a domain that contains $\mathbf{x} = \mathbf{0}$, and $D_u \subset \mathbb{R}^m$ is a domain that contains $\mathbf{u} = \mathbf{0}$. The input $\mathbf{u}(t)$ is a piecewise continuous, bounded function of t for all $t \geq 0$.

Definition 2.1.2. *A continuous function $\alpha : [0, a) \to [0, \infty)$ is said to belong to class $\mathcal{K}$ if it is strictly increasing and $\alpha(0) = 0$. It is said to belong to class $\mathcal{K}_\infty$ if $a = \infty$ and $\alpha(r) \to \infty$ as $r \to \infty$.*

Definition 2.1.3. *A continuous function $\beta : [0, \infty) \times [0, a) \to [0, \infty)$ is said to belong to class $\mathcal{KL}$ if for each fixed s, the mapping $\beta(s, r)$ belongs to class $\mathcal{K}$ with respect to r and, for each fixed r, the mapping $\beta(s, r)$ is decreasing with respect to s and $\beta(s, r) \to 0$ as $s \to \infty$.*

Definition 2.1.4. *The system (2.6) is said to be locally input–to–state stable if there exist a class $\mathcal{KL}$ function β, a class $\mathcal{K}$ function γ, and positive constants k_1 and k_2 such that for any initial state $\mathbf{x}(t_0)$ with $||\mathbf{x}(t_0)|| < k_1$ and any input*

$\mathbf{u}(t)$ *with* $\sup_{t\geq t_0} ||\mathbf{u}(t)|| < k_2$*, the solution* $\mathbf{x}(t)$ *exists and satisfies*

$$||\mathbf{x}(t)|| \leq \beta(t - t_0, ||\mathbf{x}(t_0)||) + \gamma(\sup_{t_0\leq\tau\leq t} ||\mathbf{u}(\tau)||) \tag{2.7}$$

for all $t \geq t_0 \geq 0$*. It is said to be input–to–state stable if* $D = \mathbb{R}^n, D_u = \mathbb{R}^m$*, and inequality* (2.7) *is satisfied for any initial state* $\mathbf{x}(t_0)$ *and any bounded input* $\mathbf{u}(t)$*.*

Remark 2.1.5. (2.7) *implies that for a bounded input* $\mathbf{u}(t)$*, the state* $\mathbf{x}(t)$ *will be bounded. In addition, if* $\mathbf{u}(t)$ *converges to zero as time goes to infinity in* (2.7)*, then* $\mathbf{x}(t)$ *is also convergent to zero.*

The following theorem gives a sufficient condition for input–to–state stability.

Theorem 2.1.6. *Let* $D_r = \{\mathbf{x} \in \mathbb{R}^n | \ ||\mathbf{x}|| < r\}$*,* $D_{r_u} = \{\mathbf{u} \in \mathbb{R}^m | \ ||\mathbf{u}|| < r_u\}$*, and* $\mathbf{f} : [0, \infty) \times D_r \times D_{r_u} \to \mathbb{R}^n$ *is piecewise continuous in* t *and locally Lipschitz in* $\mathbf{x}$ *and* $\mathbf{u}$*. Let* $V : [0, \infty) \times D_r \to \mathbb{R}$ *be a continuously differentiable function such that*

$$\alpha_1(||\mathbf{x}||) \leq V(t, \mathbf{x}) \leq \alpha_2(||\mathbf{x}||), \tag{2.8a}$$

$$V_t + \nabla_{\mathbf{x}} V \cdot \mathbf{f}(t, \mathbf{x}, \mathbf{u}) \leq -\alpha_3(||\mathbf{x}||), \quad \forall ||\mathbf{x}(t)|| \geq \rho(||\mathbf{u}||) > 0, \tag{2.8b}$$

$\forall (t, \mathbf{x}, \mathbf{u}) \in [0, \infty) \times D_r \times D_{r_u}$ *where* $\alpha_1, \alpha_2, \alpha_3$ *and* ρ *are class* $\mathcal{K}$ *functions. Then, the system* (2.6) *is locally input–to–state stable with* $\gamma = {\alpha_1}^{-1} \circ \alpha_2 \circ \rho$*,* $k_1 = {\alpha_2}^{-1}(\alpha_1(r))$*, and* $k_2 = \rho^{-1}(\min\{k_1, \rho(r_u)\})$*. Moreover, if* $D_r = \mathbb{R}^n, D_{r_u} = \mathbb{R}^m$*, and* α_1 *is a class* $\mathcal{K}_\infty$ *function, then the system* (2.6) *is input–to–state stable with* $\gamma = {\alpha_1}^{-1} \circ \alpha_2 \circ \rho$*. Here* γ*,* k_1*, and* k_2 *are referred in Definition 2.1.4.*

We need the following preliminaries for Lyapunov function in order to

analyze stability.

The linear time–invariant system

$$\dot{\mathbf{x}} = \mathbf{A}\mathbf{x} \tag{2.9}$$

has an equilibrium point at the origin, $\mathbf{x} \in \mathbb{R}^n$ and $\mathbf{A}$ is an $n \times n$ matrix with real components. Recall that all the eigenvalues of a *Hurwitz matrix* are negative. The origin of the system (2.9) is asymptotically stable if and only if $\mathbf{A}$ is a *Hurwitz matrix*.

Consider a quadratic Lyapunov function candidate

$$V(\mathbf{x}) = \mathbf{x}^T\mathbf{P}\mathbf{x}$$

where P is a real symmetric positive definite matrix. The derivative of V along the trajectories of the linear system (2.9) is given by

$$\dot{V}(\mathbf{x}) = \mathbf{x}^T\mathbf{P}\dot{\mathbf{x}} + \dot{\mathbf{x}}^T\mathbf{P}\mathbf{x} = \mathbf{x}^T(\mathbf{P}\mathbf{A} + \mathbf{A}^T\mathbf{P})\mathbf{x} = -\mathbf{x}^T\mathbf{Q}\mathbf{x}$$

where $\mathbf{Q}$ is a symmetric matrix defined by

$$\mathbf{P}\mathbf{A} + \mathbf{A}^T\mathbf{P} = -\mathbf{Q}. \tag{2.10}$$

(2.10) is called a Lyapunov equation. The following theorem interprets the asymptotic stability of the origin in terms of the solution of the Lyapunov equation (2.10).

Theorem 2.1.7. *An $n\times n$ matrix $\mathbf{A}$ is a Hurwitz matrix if and only if for given $n \times n$ symmetric positive definite matrix $\mathbf{Q}$ there exists an $n \times n$ symmetric positive definite matrix $\mathbf{P}$ that satisfies the equation* (2.10)*. Moreover, if $\mathbf{A}$ is a Hurwitz matrix and $\mathbf{Q}$ is a symmetric positive definite matrix, then there*

exists a unique symmetric positive definite matrix $\mathbf{P}$ *satisfying* (2.10).

The following proposition shows the system (2.2) has a stable equilibrium point. Let us denote $(I(t) - I_b)^+$ in (2.2) as the input function $u(t)$ for simple notation.

Proposition 2.1.8. *The system* (2.2) *is locally input–to–state stable in some neighborhood of* $(G(t), X(t), u(t))^T = (G_b, 0, 0)^T$. *Moreover, assume that for every* $\epsilon > 0$, *there exists* $t^*(\epsilon)$ *such that* $|I(t) - I_b| < \epsilon$ *for all* $t \geq t^*(\epsilon)$. *Then, the system* (2.2) *has a stable equilibrium point* $(G_b, 0)^T$.

Proof. In order to apply Theorem 2.1.6, we need to find a proper function V satisfying (2.8). For that purpose, we consider a system when the input function $u(t) = 0$, called the homogeneous system of (2.2), then it has an equilibrium point $(G_b, 0)^T$. The change of variable $\widetilde{G}(t) = G(t) - G_b$ transforms the homogeneous system to

$$\frac{d\widetilde{G}(t)}{dt} = -(S_G + X(t))\widetilde{G}(t) - G_b X(t), \tag{2.11a}$$

$$\frac{dX(t)}{dt} = -p_2 X(t). \tag{2.11b}$$

For the clear notation, we introduce $\widetilde{\mathbf{x}} = \begin{pmatrix} \widetilde{G}(t) \\ X(t) \end{pmatrix}$, then the linearized system of (2.11) at the zero equilibrium point is

$$\dot{\widetilde{\mathbf{x}}} = \mathbf{A}\widetilde{\mathbf{x}} + \mathbf{h}(\widetilde{\mathbf{x}}), \tag{2.12}$$

where the Jacobian matrix $\mathbf{A}$ and the nonlinear part $\mathbf{h}(\widetilde{\mathbf{x}})$ are given by

$$\mathbf{A} = \begin{pmatrix} -S_G & -G_b \\ 0 & -p_2 \end{pmatrix}, \quad \mathbf{h}(\widetilde{\mathbf{x}}) = \begin{pmatrix} -\widetilde{G}(t)X(t) \\ 0 \end{pmatrix}.$$

Since $\mathbf{A}$ has negative eigenvalues $-S_G$ and $-p_2$, the linear system $\dot{\widetilde{\mathbf{x}}} = \mathbf{A}\widetilde{\mathbf{x}}$ has an asymptotically stable equilibrium point at the origin.

From Theorem 2.1.7, a symmetric positive definite matrix $\mathbf{P}$, the solution of the following equation

$$\mathbf{PA} + \mathbf{A}^T\mathbf{P} = -\mathbf{I} \text{ (} 2 \times 2 \text{ identity matrix)}$$

is given by

$$\mathbf{P} = \frac{1}{2S_G} \begin{pmatrix} 1 & -\frac{G_b}{S_G+p_2} \\ -\frac{G_b}{S_G+p_2} & \frac{S_G(S_G+p_2)+{G_b}^2}{p_2(S_G+p_2)} \end{pmatrix}.$$

For the linear system $\dot{\widetilde{\mathbf{x}}} = \mathbf{A}\widetilde{\mathbf{x}}$, we consider the Lyapunov function $V(\widetilde{\mathbf{x}}) = \widetilde{\mathbf{x}}^T\mathbf{P}\widetilde{\mathbf{x}}$.

Then we have

$$\begin{aligned} \lambda_{min}(\mathbf{P})||\widetilde{\mathbf{x}}||^2 &\leq V(\widetilde{\mathbf{x}}) \leq \lambda_{max}(\mathbf{P})||\widetilde{\mathbf{x}}||^2, && \text{(2.13a)} \\ \nabla_{\widetilde{\mathbf{x}}}V \cdot \mathbf{A}\widetilde{\mathbf{x}} = -\widetilde{\mathbf{x}}^T\mathbf{I}\widetilde{\mathbf{x}} &\leq -\lambda_{min}(\mathbf{I})||\widetilde{\mathbf{x}}||^2 = -||\widetilde{\mathbf{x}}||^2, && \text{(2.13b)} \\ ||\nabla_{\widetilde{\mathbf{x}}}V|| = ||2\widetilde{\mathbf{x}}^T\mathbf{P}|| &\leq 2||\mathbf{P}||\,||\widetilde{\mathbf{x}}|| = 2\lambda_{max}(\mathbf{P})||\widetilde{\mathbf{x}}||, && \text{(2.13c)} \end{aligned}$$

where $\lambda_{min}(\mathbf{P})$ and $\lambda_{max}(\mathbf{P})$ denote the positive minimum and maximum eigenvalues of matrix $\mathbf{P}$, respectively.

Let us split the system (2.2) by

$$\dot{\widetilde{\mathbf{x}}} = \mathbf{A}\widetilde{\mathbf{x}} + \mathbf{h}(\widetilde{\mathbf{x}}) + \mathbf{g}(u(t)), \tag{2.14}$$

where $\mathbf{g}(u(t))$ with the input function $u(t)$ is given by

$$\mathbf{g}(u(t)) = \begin{pmatrix} 0 \\ p_2 S_I u(t) \end{pmatrix}.$$

Now, we are going to show that the Lyapunov function $V(\widetilde{\mathbf{x}})$ for the linear system $\dot{\widetilde{\mathbf{x}}} = \mathbf{A}\widetilde{\mathbf{x}}$ is indeed the proper function for the system (2.14) satisfying (2.8).

By using (2.13b), we obtain

$$\dot{V}(\widetilde{\mathbf{x}}) = \nabla_{\widetilde{\mathbf{x}}} V \cdot \dot{\widetilde{\mathbf{x}}} \leq -||\widetilde{\mathbf{x}}||^2 + ||\nabla_{\widetilde{\mathbf{x}}} V||\ ||\mathbf{h}(\widetilde{\mathbf{x}})|| + ||\nabla_{\widetilde{\mathbf{x}}} V||\ ||\mathbf{g}(u(t))||. \quad (2.15)$$

By the Cauchy–Schwarz inequality, the nonlinear part $\mathbf{h}(\widetilde{\mathbf{x}})$ is bounded as follows:

$$||\mathbf{h}(\widetilde{\mathbf{x}})|| \leq \frac{1}{2}||\widetilde{\mathbf{x}}||^2. \quad (2.16)$$

In addition, $\mathbf{g}(u(t))$ with the input function $u(t)$ satisfies the following equality

$$||\mathbf{g}(u(t))|| = p_2 S_I ||u(t)||. \quad (2.17)$$

Substituting (2.16) and (2.17) into (2.15), and using the inequality (2.13c), we obtain

$$\dot{V}(\widetilde{\mathbf{x}}) \leq -||\widetilde{\mathbf{x}}||^2 + \lambda_{max}(\mathbf{P})||\widetilde{\mathbf{x}}||^3 + 2\lambda_{max}(\mathbf{P}) p_2 S_I ||\widetilde{\mathbf{x}}||\ ||u(t)||. \quad (2.18)$$

Let $D_{r_u} = \{u(t) \in \mathbb{R} |\ ||u(t)|| < r_u\}$ and $D_r = \{\widetilde{\mathbf{x}} \in \mathbb{R}^2 |\ ||\widetilde{\mathbf{x}}|| < r\}$, and choose the constants r_u and r satisfying

$$0 < r_u < \frac{\lambda_{min}(\mathbf{P})\theta^2}{8{\lambda_{max}}^3(\mathbf{P}) p_2 S_I}, \quad 0 < \theta < 1, \quad (2.19a)$$

$$r < \frac{1}{\lambda_{max}(\mathbf{P})}, \quad (2.19b)$$

$$\left(\frac{2\lambda_{max}(\mathbf{P}) p_2 S_I r\, r_u}{\theta(1 - \lambda_{max}(\mathbf{P}) r)}\right)^{1/2} < r\left(\frac{\lambda_{min}(\mathbf{P})}{\lambda_{max}(\mathbf{P})}\right)^{1/2}. \quad (2.19c)$$

(2.19) will be needed to estimate the bounds on the initial state and input

(the constants k_1 and k_2) in Definition 2.1.4 and Theorem 2.1.6.

By simple calculation,(2.19b) and (2.19c) become

$$r_1 < r < \min\left(r_2, \frac{1}{\lambda_{max}(\mathbf{P})}\right) = r_2, \tag{2.20}$$

where

$$\begin{aligned} r_1 &= \frac{\lambda_{min}(\mathbf{P})\theta - \sqrt{(\lambda_{min}(\mathbf{P})\theta)^2 - 8{\lambda_{max}}^3(\mathbf{P})\lambda_{min}(\mathbf{P})p_2 S_I r_u}}{2\lambda_{min}(\mathbf{P})\lambda_{max}(\mathbf{P})\theta}, \\ r_2 &= \frac{\lambda_{min}(\mathbf{P})\theta + \sqrt{(\lambda_{min}(\mathbf{P})\theta)^2 - 8{\lambda_{max}}^3(\mathbf{P})\lambda_{min}(\mathbf{P})p_2 S_I r_u}}{2\lambda_{min}(\mathbf{P})\lambda_{max}(\mathbf{P})\theta}. \end{aligned}$$

By recalling (2.18), we get

$$\begin{aligned} \dot{V}(\widetilde{\mathbf{x}}) \leq & -(1-\lambda_{max}(\mathbf{P})r)||\widetilde{\mathbf{x}}||^2 + 2\lambda_{max}(\mathbf{P})p_2 S_I r||u(t)|| \\ = & -(1-\theta)(1-\lambda_{max}(\mathbf{P})r)||\widetilde{\mathbf{x}}||^2 - \theta(1-\lambda_{max}(\mathbf{P})r)||\widetilde{\mathbf{x}}||^2 \\ & + 2\lambda_{max}(\mathbf{P})p_2 S_I r||u(t)||, \quad (0<\theta<1) \\ \leq & -(1-\theta)(1-\lambda_{max}(\mathbf{P})r)||\widetilde{\mathbf{x}}||^2, \end{aligned} \tag{2.21}$$

where $\left(\frac{2\lambda_{max}(\mathbf{P})p_2 S_I r||u(t)||}{\theta(1-\lambda_{max}(\mathbf{P})r)}\right)^{1/2} \leq ||\widetilde{\mathbf{x}}|| < r$.

From (2.13a) and (2.21), we finally find the explicit forms of class $\mathcal{K}$ functions on $D_r \times D_{r_u}$,

$$\begin{aligned} \alpha_1(||\widetilde{\mathbf{x}}||) =& \lambda_{min}(\mathbf{P})||\widetilde{\mathbf{x}}||^2, \\ \alpha_2(||\widetilde{\mathbf{x}}||) =& \lambda_{max}(\mathbf{P})||\widetilde{\mathbf{x}}||^2, \\ \alpha_3(||\widetilde{\mathbf{x}}||) =& (1-\theta)(1-\lambda_{max}(\mathbf{P})r)||\widetilde{\mathbf{x}}||^2, \\ \rho(||u||) =& \left(\frac{2\lambda_{max}(\mathbf{P})p_2 S_I r||u||}{\theta(1-\lambda_{max}(\mathbf{P})r)}\right)^{1/2}. \end{aligned}$$

Therefore, the system (2.14) is locally input–to–state stable by Theo-

rem 2.1.6 with

$$\begin{aligned} k_1 =& {\alpha_2}^{-1}(\alpha_1(r)) = r\left(\frac{\lambda_{min}(\mathbf{P})}{\lambda_{max}(\mathbf{P})}\right)^{1/2}, \\ k_2 =& \rho^{-1}(\min\{k_1, \rho(r_u)\}) = r_u, \\ \gamma(a) =& {\alpha_1}^{-1} \circ \alpha_2 \circ \rho(a) = \left(\frac{2{\lambda_{max}}^2(\mathbf{P})p_2 S_I r a}{\lambda_{min}(\mathbf{P})\theta(1-\lambda_{max}(\mathbf{P})r)}\right)^{1/2}. \end{aligned}$$

Note that the condition (2.19c) of choosing r is equivalent to $\frac{k_1}{\rho(r_u)} > 1$. By the assumption, the input function $u(t) = (I(t) - I_b)^+$ converges to zero for all $t \geq t^*(\epsilon)$. Therefore, from Remark 2.1.5, we proved the system (2.14) has a stable equilibrium point $(G_b, 0)^T$, which is also a stable equilibrium point in the homogeneous system of (2.14). □

2.1.3 Lipolysis model

In 2008, Periwal *et al.* [79] developed the lipolysis model for describing the effects of insulin on the suppression of lipolysis. In this model, lipolysis was suppressed by insulin through a remote compartment acting on both glucose and FFA simultaneously. This process can be described by the following system of ordinary differential equations.

$$\begin{aligned} \frac{dG(t)}{dt} &= -(S_G + S_I X(t))G(t) + S_G G_b, \quad G(t_0) = G_{t_0}, && \text{(2.22a)} \\ \frac{dX(t)}{dt} &= c_x(I(t) - X(t) - I_b), \quad X(t_0) = X_{t_0}, && \text{(2.22b)} \\ \frac{dF(t)}{dt} &= l_0 + \frac{l_2}{1 + \left(\frac{X(t)}{X_2}\right)^m} - c_f F(t), \quad F(t_0) = F_{t_0}, && \text{(2.22c)} \end{aligned}$$

where

- $F(t)$ $[\mu M]$ is the FFA concentration at time t $[min]$;

- $X(t)$ $[\mu U/ml]$ is the effect of insulin in a remote glucose;
- c_x $[min^{-1}]$ is the rate of influx and outflux for insulin in $X(t)$;
- l_0 $[\mu M/min^{-1}]$ is the minimal lipolysis rate;
- $l_2 + l_0$ is the maximal lipolysis rate;
- X_2 and m are the Hill constant and coefficient, respectively;
- c_f $[min^{-1}]$ is the first–order reaction rate for clearing FFA.

The variables $G(t)$, $I(t)$ and the parameters S_G, G_b, S_I, and I_b in (2.22) are identical to those of MINMOD Millennium. In (2.22c), $l_0 + \dfrac{l_2}{1 + (X(t)/X_2)^m}$ is called the Hill function. This measures the insulin–dependent rate of lipolysis, and models the insulin–suppressible plasma FFA input flux (see, for instance, [47] for more details.)

In this model, $I(t)$ is an input variable whose data are obtained from IM–FSIGT, whereas $G(t)$, $X(t)$, and $F(t)$ are output variables. And we consider $I(t)$ to be bounded and piecewise C^1 function. During the experiment, data before time t_0 are ignored due to the rapid changes in the early stages of the model.

We are going to prove the positivity, boundedness, and stability of solutions on (2.22).

Proposition 2.1.9. *Let $G(t), X(t), I(t)$, and $F(t)$ satisfy (2.22). Then, $G(t)$ is positive for all $t > t_0$. If $I(t) \geq I_b$ for all $t \geq t_0$, then $X(t)$ and $F(t)$ are also positive for all $t > t_0$. Moreover, we have*

$$X(t) \geq e^{-c_x(t-t_0)} X_{t_0}, \tag{2.23a}$$

$$\nu(t) \leq F(t) \leq \nu(t) + l_2 \int_{t_0}^{t} e^{-c_f(t-u)} \left(1 + \left(\frac{X_{t_0}}{X_2}\right)^m e^{c_x(t_0-u)m}\right)^{-1} du, \tag{2.23b}$$

where $\nu(t) = e^{-c_f(t-t_0)}F_{t_0} + \left(1 - e^{-c_f(t-t_0)}\right)\dfrac{l_0}{c_f}$.
We also have

$$\limsup_{t\to\infty} \; G(t) \le G_b. \tag{2.24}$$

In particular, if $X_{t_0} = 0$, *then*

$$\limsup_{t\to\infty} \; F(t) \le \frac{l_0 + l_2}{c_f}. \tag{2.25}$$

Proof. By introducing an integrating factor $\mu(t) = e^{\int_{t_0}^{t}(S_G + S_I X(u))\,du}$, the solution of the system (2.22) can be found:

$$\begin{aligned}
G(t) =& \frac{1}{\mu(t)}\left(G_{t_0} + S_G G_b \int_{t_0}^{t} \mu(u)\; du\right),\\
X(t) =& e^{-c_x(t-t_0)}X_{t_0} + c_x\int_{t_0}^{t} e^{-c_x(t-u)}[I(u) - I_b]\; du,\\
F(t) =& e^{-c_f(t-t_0)}F_{t_0} + \int_{t_0}^{t} e^{-c_f(t-u)}\left(l_0 + \frac{l_2}{1 + \left(\frac{X(u)}{X_2}\right)^m}\right)\; du.
\end{aligned}$$

The positivity of $G(t)$ follows immediately. The assumption $I(t) \ge I_b$ for all $t \ge t_0$ implies the positivity of $X(t)$, and therefore that of $F(t)$, for all $t > t_0$. (2.23a) also follows from the solution form.

From (2.22c) and (2.23a), we have

$$l_0 \le \frac{dF}{dt}(t) + c_f F(t) \le l_0 + l_2\left(1 + \left(\frac{e^{-c_x(t-t_0)}X_{t_0}}{X_2}\right)^m\right)^{-1}. \tag{2.26}$$

Multiplying by $e^{c_f t}$ in (2.26) and integrating over $[t_0, t]$, we get

$$\nu(t) \le F(t) \le \nu(t) + l_2\int_{t_0}^{t} e^{-c_f(t-u)}\left(1 + \left(\frac{X_{t_0}}{X_2}\right)^m e^{c_x(t_0-u)m}\right)^{-1} du,$$

where $\nu(t) = e^{-c_f(t-t_0)}F_{t_0} + \left(1 - e^{-c_f(t-t_0)}\right)\dfrac{l_0}{c_f}$.

By applying a similar proof as for (2.5), (2.24) is completed. From (2.23b), we obtain (2.25). □

In this model (2.22), let us denote $(I(t) - I_b)$ as the input function $u(t)$ for simple notation.

Proposition 2.1.10. *The system* (2.22) *is locally input–to–state stable in some neighborhood of* $(G(t), X(t), F(t), u(t))^T = (G_b, 0, (l_0 + l_f)/c_f, 0)^T$ *when* $m > 1$. *In addition, assume that for every* $\epsilon > 0$, *there exists* $t^*(\epsilon)$ *such that* $|I(t) - I_b| < \epsilon$ *for all* $t \geq t^*(\epsilon)$. *Then, the system* (2.22) *has a stable equilibrium point* $(G_b, 0, (l_0 + l_f)/c_f)^T$.

Proof. In order to apply Theorem 2.1.6, a proper function V satisfying (2.8) is required. For that purpose, we consider a system when the input function $u(t) = 0$, called the homogeneous system of (2.22). An equilibrium point $(G_b, 0, (l_0 + l_2)/c_f)^T$ of the homogeneous system for (2.22) is obtained by setting the right–hand sides to be zero.

By using the change of variables

$$\widetilde{G}(t) = G(t) - G_b, \quad \widetilde{F}(t) = F(t) - \frac{l_0 + l_2}{c_f},$$

the homogeneous system becomes

$$\begin{aligned}
\frac{d\widetilde{G}(t)}{dt} &= -(S_G + S_I X(t))\widetilde{G}(t) - S_I G_b X(t), && \text{(2.27a)}\\
\frac{dX(t)}{dt} &= -c_x X(t), && \text{(2.27b)}\\
\frac{d\widetilde{F}(t)}{dt} &= l_2 \left(1 + \left(\frac{X(t)}{X_2}\right)^m\right)^{-1} - c_f \widetilde{F}(t) - l_2. && \text{(2.27c)}
\end{aligned}$$

For the clear notation, we introduce $\widetilde{\mathbf{x}} = \begin{pmatrix} \widetilde{G}(t) \\ X(t) \\ \widetilde{F}(t) \end{pmatrix}$, then the linearized system of (2.27) at the zero equilibrium point can be expressed as

$$\dot{\widetilde{\mathbf{x}}} = \mathbf{A}\widetilde{\mathbf{x}} + \mathbf{h}(\widetilde{\mathbf{x}}), \tag{2.28}$$

where the Jacobian matrix $\mathbf{A}$ and the nonlinear part $\mathbf{h}(\widetilde{\mathbf{x}})$ are given by

$$\mathbf{A} = \begin{pmatrix} -S_G & -S_I G_b & 0 \\ 0 & -c_x & 0 \\ 0 & 0 & -c_f \end{pmatrix}, \quad \mathbf{h}(\widetilde{\mathbf{x}}) = \begin{pmatrix} -S_I X(t)\widetilde{G}(t) \\ 0 \\ l_2 \left(1 + \left(\frac{X(t)}{X_2}\right)^m\right)^{-1} - l_2 \end{pmatrix}.$$

Since $\mathbf{A}$ has negative eigenvalues $-S_G$, $-c_x$, and $-c_f$, the zero equilibrium point of the linear system $\dot{\widetilde{\mathbf{x}}} = \mathbf{A}\widetilde{\mathbf{x}}$ is uniformly asymptotically stable.

Theorem 2.1.7 gives a symmetric positive definite matrix $\mathbf{P}$ which is the solution of the following equation

$$\mathbf{P}\mathbf{A} + \mathbf{A}^T\mathbf{P} = -\mathbf{I} \ (3 \times 3 \text{ identity matrix})$$

is given by

$$\mathbf{P} = \begin{pmatrix} \frac{1}{2S_G} & -\frac{S_I G_b}{2S_G(S_G+c_x)} & S_G + c_f \\ -\frac{S_I G_b}{2S_G(S_G+c_x)} & \frac{(S_I G_b)^2}{2S_G c_x(S_G+c_x)} & -\frac{S_I G_b(S_G+c_f)}{c_x+c_f} \\ S_G + c_f & -\frac{S_I G_b(S_G+c_f)}{c_x+c_f} & \frac{1}{2c_f} \end{pmatrix}.$$

For the linear system $\dot{\widetilde{\mathbf{x}}} = \mathbf{A}\widetilde{\mathbf{x}}$, we consider the Lyapunov function $V(\widetilde{\mathbf{x}}) = \widetilde{\mathbf{x}}^T\mathbf{P}\widetilde{\mathbf{x}}$, then we have the inequalities in (2.13).

Let us split the system (2.22) by

$$\dot{\widetilde{\mathbf{x}}} = \mathbf{A}\widetilde{\mathbf{x}} + \mathbf{h}(\widetilde{\mathbf{x}}) + \mathbf{g}(u(t)), \tag{2.29}$$

where $\mathbf{g}(u(t))$ with the input function $u(t)$ is given by

$$\mathbf{g}(u(t)) = \begin{pmatrix} 0 \\ c_x u(t) \\ 0 \end{pmatrix}.$$

Now, we are going to show that the Lyapunov function $V(\widetilde{\mathbf{x}})$ for the linear system $\dot{\widetilde{\mathbf{x}}} = \mathbf{A}\widetilde{\mathbf{x}}$ is indeed the proper function for the system (2.29) satisfying (2.8).

By using (2.13b), we have

$$\dot{V}(\widetilde{\mathbf{x}}) = \nabla_{\widetilde{\mathbf{x}}} V \cdot \dot{\widetilde{\mathbf{x}}} \leq -||\widetilde{\mathbf{x}}||^2 + ||\nabla_{\widetilde{\mathbf{x}}} V||\ ||\mathbf{h}(\widetilde{\mathbf{x}})|| + ||\nabla_{\widetilde{\mathbf{x}}} V||\ ||\mathbf{g}(u(t))||. \tag{2.30}$$

Since the nonlinear part $\mathbf{h}(\widetilde{\mathbf{x}})$ satisfies $\lim_{||\widetilde{\mathbf{x}}||\to 0} ||\mathbf{h}(\widetilde{\mathbf{x}})|| = 0$, for any $\epsilon > 0$, there exists a constant $r > 0$ such that

$$||\mathbf{h}(\widetilde{\mathbf{x}})|| < \epsilon \quad \text{as} \quad ||\widetilde{\mathbf{x}}(t)|| < r. \tag{2.31}$$

Moreover, $\mathbf{g}(u(t))$ with the input function $u(t)$ satisfies

$$||\mathbf{g}(u(t))|| = c_x ||u(t)||. \tag{2.32}$$

Applying (2.31) and (2.32) into (2.30), and using the inequality (2.13c), we get

$$\dot{V}(\widetilde{\mathbf{x}}) \leq -||\widetilde{\mathbf{x}}||^2 + 2\lambda_{max}(\mathbf{P})\,\epsilon\,||\widetilde{\mathbf{x}}|| + 2\lambda_{max}(\mathbf{P})\,c_x\,||u(t)||\ ||\widetilde{\mathbf{x}}|| \tag{2.33}$$

Let $D_{r_u} = \{u(t) \in \mathbb{R} |\ ||u(t)|| < r_u\}$ and $D_r = \{\widetilde{\mathbf{x}} \in \mathbb{R}^3 |\ ||\widetilde{\mathbf{x}}|| < r\}$.

We choose a sufficiently small constant $r_u > 0$, and consider a constant r such that $r > (\epsilon + c_x r_u)\frac{2\lambda_{max}(\mathbf{P})}{\theta}\left(\frac{\lambda_{max}(\mathbf{P})}{\lambda_{min}(\mathbf{P})}\right)^{1/2}$, $0 < \theta < 1$, in order to estimate the bounds on the initial state and input (the constants k_1 and k_2) in Definition 2.1.4 and Theorem 2.1.6.

By recalling (2.33), we obtain

$$\begin{aligned}\dot{V}(\widetilde{\mathbf{x}}) =& -(1-\theta)||\widetilde{\mathbf{x}}||^2 - \theta||\widetilde{\mathbf{x}}||^2 \\ &+ (2\lambda_{max}(\mathbf{P})\,\epsilon + 2\lambda_{max}(\mathbf{P})\,c_x\,||u(t)||)\,||\widetilde{\mathbf{x}}||, \quad (0<\theta<1) \\ \leq& -(1-\theta)||\widetilde{\mathbf{x}}||^2, \quad \frac{2\lambda_{max}(\mathbf{P})\,\epsilon + 2\lambda_{max}(\mathbf{P})\,c_x\,||u(t)||}{\theta} \leq ||\widetilde{\mathbf{x}}|| < r.\end{aligned} \tag{2.34}$$

From (2.13a) and (2.34), we finally get the explicit forms of the class $\mathcal{K}$ functions on $D_r \times D_{r_u}$,

$$\begin{aligned}\alpha_1(||\widetilde{\mathbf{x}}||) =& \lambda_{min}(\mathbf{P})||\widetilde{\mathbf{x}}||^2, \\ \alpha_2(||\widetilde{\mathbf{x}}||) =& \lambda_{max}(\mathbf{P})||\widetilde{\mathbf{x}}||^2, \\ \alpha_3(||\widetilde{\mathbf{x}}||) =& (1-\theta)||\widetilde{\mathbf{x}}||^2, \\ \rho(||u||) =& \frac{2\lambda_{max}(\mathbf{P})\,\epsilon + 2\lambda_{max}(\mathbf{P})\,c_x\,||u||}{\theta}.\end{aligned}$$

Therefore, by Theorem 2.1.6, the system (2.29) is locally input–to–state stable with

$$\begin{aligned}k_1 =& {\alpha_2}^{-1}(\alpha_1(r)) = r\left(\frac{\lambda_{min}(\mathbf{P})}{\lambda_{max}(\mathbf{P})}\right)^{1/2}, \\ k_2 =& \rho^{-1}(\min\{k_1, \rho(r_u)\}) = r_u, \\ \gamma(a) =& {\alpha_1}^{-1} \circ \alpha_2 \circ \rho(a) = \frac{2\lambda_{max}(\mathbf{P})\,\epsilon + 2\lambda_{max}(\mathbf{P})\,c_x\,a}{\theta}.\end{aligned}$$

Note that the condition of choosing r is equivalent to $\frac{k_1}{\rho(r_u)} > 1$.

Moreover, by the assumption and Remark 2.1.5, the system (2.29) has a stable equilibrium point $(G_b, 0, l_0 + l_f/c_f)^T$, which is also a stable equilibrium point in homogeneous system of (2.29). This proves the proposition. □

2.1.4 Numerical methods

To estimate insulin sensitivity (S_I) and glucose effectiveness (S_G), we have used the fourth–order Runge–Kutta method [16] to solve the glucose–insulin dynamics, the nonlinear weighted least–squares method [63] to minimize the objective functional, and the Levenberg–Marquardt algorithm [41] to estimate parameter values. We have applied these numerical methods to solve MINMOD, Arino's minimal model, MINMOD Millennium, and the lipolysis model. The experimental data used for MINMOD, Arino's minimal model, and MINMOD Millennium were extracted from [76]. For the lipolysis model, we used data in [79]. We have simulated the glucose–insulin dynamics using two approaches. In the first approach, for MINMOD and Arino's minimal model, we combined glucose disappearance and the insulin kinetics model to consider the feedback system of glucose–insulin. Thus, we solved the system of differential equations with three variables simultaneously. In the second approach, we divided the glucose–insulin dynamics into systems of glucose disappearance and insulin kinetics, as discussed in [76]. In the second approach, the linearly interpolated plasma insulin (glucose) concentration plays the role of input data for the glucose disappearance model (insulin kinetics model). MINMOD Millennium and the lipolysis model are only used to simulate the glucose disappearance model. Flow charts illustrating these two approaches are shown in Figure 2.1a and Figure 2.1b.

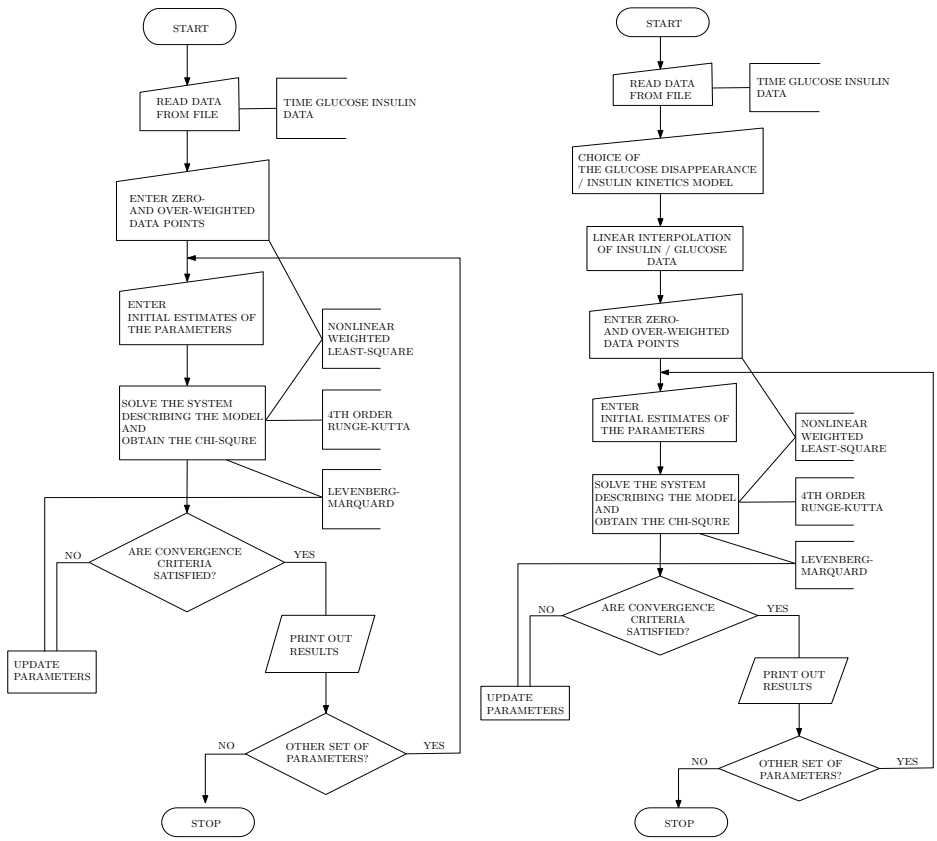

(a) The first approach. (b) The second approach.

Figure 2.1: Numerical methods.

2.2 Parameter estimation

As we have observed, the glucose–insulin mathematical model is a system of differential equations with a set of parameters. Mathematical problems with such parameter–dependent differential equations can be categorized into forward and inverse problems. Forward problems need analysis and model simulations for given parameter values, whereas inverse problems require parameter estimation based on the measurements of output variables. Among various important problems related to parameter estimation, we are partic-

ularly interested in finding the parameter set that minimizes the chi–square value between the observed data in [76, 79] and the numerical solutions.

2.2.1 Parameter sensitivity

To estimate parameters in the inverse problems, we use the Levenberg–Marquardt algorithm [41], which is based on Newton's method. When we use Newton–type methods for approximating some quantities, it is important to give reasonable initial guesses, so that the observed data fits the model correctly. Also, it often happens that parameters of minor importance have a large impact on the model. In such cases, models could lose their validity and reliability. Hence, we need to determine the sensitivity of parameters to improve the goodness of fit and validity. In this subsection, we perform a parameter sensitivity analysis using the semi–relative sensitivity [90].

Let me define $\bar{y}$ as the quantity obtained from the numerical simulation. We want to measure the relative sensitivity of $\bar{y}$ to a set of parameters $\vec{a} = (a_i)_{i=1}^m$. The semi–relative sensitivity of $\bar{y}$ to a particular parameter a_i is given by

$$\frac{\partial \bar{y}(t;\vec{a})}{\partial a_i} \cdot a_i. \tag{2.35}$$

This is computed by differentiating the given ODE model

$$\frac{d\bar{y}}{dt} = f(t, \bar{y}; \vec{a}), \quad \bar{y}(t_0) = y_0, \tag{2.36}$$

with respect to a_i and interchanging the order of time and parameter derivatives. This process provides sensitivity information as a function of time over the interval of interest. In case we need some overall measure of the sensitivity of the solution to the parameters, we take a continuous L_2 norm and then rank the resulting scalars to determine the most sensitive parameter. The relative

l_2 error is calculated by

$$\frac{\sqrt{\chi^2}}{\sqrt{\sum_{i=1}^{n} {y_i}^2}}, \tag{2.37}$$

where $\chi^2 = \sum_{i=1}^{n}(y_i - \bar{y}(t_i; \vec{a}))^2/{\sigma_i}^2$ is the chi–square value, n is the number of data, y_i is the observed datum at time t_i, and σ_i is the standard deviation associated with each measurement y_i.

2.2.2 Analysis of parameter sensitivity

In this subsection, we present and analyze the parameter sensitivity results for MINMOD, Arino's minimal model, MINMOD Millennium, and the lipolysis model. Parameter sensitivity analyses for MINMOD–glucose disappearance, MINMOD–insulin kinetics, and Arino–insulin kinetics are also performed. The data set used for this analysis was obtained from [76, 79].

MINMOD

The estimated parameter set in MINMOD is composed of S_G, p_2, S_I, n, γ, h, G_0, and I_0. For details of the equations and parameters, see [76]. Among these eight parameters, we want to find the most sensitive parameter using the semi–relative sensitivity analysis. We have used relative weights of 0 or 1 for the plasma glucose–insulin levels when we apply the nonlinear weighted least–squares method [63] to minimize the objective functional (2.37). The weights for the observed data at 0 and 2 min were set to 0 for the parameter estimation, and the initial guesses for S_G, G_0, n, and I_0 were chosen using a linear regression of log–transformed data, as in [76]. The initial guesses for p_2, S_I, and γ were set to typical values for consistency with normal values in humans [7]. The basal glucose value was assigned to the initial guess for h. Table 2.1 lists the estimated values, initial guesses of the parameters, and the relative l_2 error.

Parameter	S_G	p_2	S_I	n	γ	h	G_0	I_0
Estimated	0.37470e−01	0.57504e−02	0.65490e−03	0.22236	0.32386e−02	79.165	302.24	300.08
Initial	0.38271e−01	0.20000e−01	0.50000e−03	0.23393	0.28000e−02	92.000	325.29	336.15

Table 2.1: Estimated parameters for MINMOD.
Relative l_2 error: 4.56e−02.

	Glucose states		Insulin states	
Rank	Parameter a_i	$\|\|\partial G(t)/\partial a_i\|\|_2$	Parameter a_i	$\|\|\partial I(t)/\partial a_i\|\|_2$
1	S_I	0.1981e+06	S_I	0.1896e+06
2	γ	0.2214e+05	γ	0.5350e+05
3	p_2	0.1857e+05	p_2	0.1532e+05
4	S_G	0.1101e+05	S_G	0.6969e+04
5	n	0.6572e+03	n	0.1538e+04
6	h	0.4482e+01	h	0.1184e+02
7	G_0	0.2917e+01	G_0	0.7960e+00
8	I_0	0.3249e+00	I_0	0.6804e+00

Table 2.2: Glucose and insulin ranking with L_2 norm for MINMOD.

In glucose–insulin dynamics, the ability to dispose of carbohydrate depends on the responsiveness of the pancreatic β-cells to glucose and insulin sensitivity [7]. In MINMOD, we are able to generate characteristic parameters for insulin sensitivity and pancreatic responsivity. Insulin sensitivity (S_I) can be calculated from the glucose disappearance model, and we can use the insulin kinetics model to estimate parameters for pancreatic responsivity, which describes the first phase insulin release (n) and the second phase insulin secretion (γ). From Table 2.2, we can verify that S_I and γ are the two most sensitive parameters, which agrees with the underlying physiological phenomena.

We also performed a semi–relative sensitivity analysis for MINMOD–glucose disappearance and MINMOD–insulin kinetics. In particular, to improve the numerical fit for the parameter estimation of MINMOD–insulin kinetics, we set the weights for the observed data at 4, 6, and 8 min to be 10. Table 2.3 and

Table 2.5 give the estimated values, initial guesses of the parameters, and the relative l_2 errors for MINMOD–glucose disappearance and MINMOD–insulin kinetics, respectively. We can also observe that S_I and γ are the most sensitive parameters in each model from Table 2.4 and Table 2.6.

Parameter	S_G	p_2	S_I	G_0
Estimated	0.20417e−01	0.29268e−01	0.57327e−03	264.88
Initial	0.38271e−01	0.20000e−01	0.50000e−03	325.29

Table 2.3: Estimated parameters for MINMOD–glucose disappearance. Relative l_2 error: 2.66e−02.

	Glucose states	
Rank	Parameter a_i	$\|\|\partial G(t)/\partial a_i\|\|_2$
1	S_I	0.5790e+06
2	S_G	0.1360e+05
3	p_2	0.5444e+04
4	G_0	0.3382e+01

Table 2.4: Glucose ranking with L_2 norm for MINMOD–glucose disappearance model.

Parameter	n	γ	h	I_0
Estimated	0.25922	0.34871e−02	79.435	354.31
Initial	0.23393	0.28000e−02	92.000	336.15

Table 2.5: Estimated parameters for MINMOD–insulin kinetics model. Relative l_2 error: 8.89e−02.

Arino's minimal model

For details of Arino's minimal model, see [25]. We perform a semi–relative sensitivity analysis for Arino's minimal model with the same data set used in MINMOD. The parameter set is identical to that of MINMOD. Table 2.7

	Insulin states	
Rank	Parameter a_i	$\|\|\partial I(t)/\partial a_i\|\|_2$
1	γ	0.5729e+05
2	n	0.1408e+04
3	h	0.1850e+02
4	I_0	0.5137e+00

Table 2.6: Insulin ranking with L_2 norm for MINMOD–insulin kinetics model.

shows the estimated values, initial guesses of the parameters, and the relative l_2 error. Table 2.8 shows that S_I and γ are again the most sensitive param-

Parameter	S_G	p_2	S_I	n	γ	h	G_0	I_0
Estimated	0.31734e−01	0.13145e−01	0.46137e−03	0.25139	0.33087e−02	90.053	296.69	321.39
Initial	0.38271e−01	0.20000e−01	0.50000e−03	0.23393	0.28000e−02	92.000	325.29	336.15

Table 2.7: Estimated parameters for Arino's minimal model.
Relative l_2 error : 4.32e−02.

eters, as in MINMOD. In the case of the Arino–insulin kinetics model, which

	Glucose states		Insulin states	
Rank	Parameter a_i	$\|\|\partial G(t)/\partial a_i\|\|_2$	Parameter a_i	$\|\|\partial I(t)/\partial a_i\|\|_2$
1	S_I	0.4053e+06	S_I	0.1797e+06
2	γ	0.2021e+05	γ	0.3666e+05
3	S_G	0.1162e+05	p_2	0.4590e+04
4	p_2	0.1008e+05	S_G	0.4518e+04
5	n	0.6981e+03	n	0.1192e+04
6	G_0	0.3067e+01	h	0.3540e+01
7	h	0.1952e+01	G_0	0.7181e+00
8	I_0	0.4114e+00	I_0	0.5638e+00

Table 2.8: Glucose and insulin ranking with L_2 norm for Arino's minimal model.

only considers insulin dynamics with interpolated glucose data, the estimated values, initial guesses of the parameters, and the relative l_2 error are shown in

Table 2.9. The weights are identical to those in the MINMOD–insulin kinetics model. As expected, the pancreatic responsivity parameters (n and γ) are the two most sensitive parameters.

Parameter	n	γ	h	I_0
Estimated	0.29224	0.44601e−02	102.02	380.69
Initial	0.23393	0.28000e−02	92.000	336.15

Table 2.9: Estimated parameters for Arino–insulin kinetics model. Relative l_2 error: 6.44e−02.

	Glucose states	
Rank	Parameter a_i	$\|\|\partial I(t)/\partial a_i\|\|_2$
1	γ	0.2911e+05
2	n	0.1100e+04
3	h	0.3438e+01
4	I_0	0.4284e+00

Table 2.10: Insulin ranking with L_2 norm for Arino–insulin kinetics model.

MINMOD Millennium

We performed a semi–relative sensitivity analysis for MINMOD Millennium. In MINMOD Millennium, the estimated parameter set is composed of S_G, p_2, S_I, and G_0. When we applied the nonlinear weighted least–squares method to minimize the objective functional [63], the first four observed glucose data were excluded by setting their weights to zero. For the parameter estimation, the initial guesses for glucose (G_0) and glucose effectivity (S_G) were chosen by a linear regression of six log–transformed data points after 8 min [13]. The initial guesses for p_2 and S_I were set to typical values for consistency with human physiology [68]. In particular, in order to address the "changing baseline" phenomenon to produce acceptable results describing the

glucose profile, G_b was obtained from a baseline correction determined by the existence of several data and pre–injection value [13]. Table 2.11 lists the estimated parameter values, initial guesses of the parameters, and the relative l_2 error.

Parameter	S_G	p_2	S_I	G_0
Estimated	0.21120e−01	0.30710e−01	0.52790e−03	266.38
Initial	0.18841e−01	0.50600e−01	0.41500e−03	268.40

Table 2.11: Estimated parameters for MINMOD Millennium.
Relative l_2 error: 2.75e−02.

	Glucose states	
Rank	Parameter a_i	$\|\|\partial G(t)/\partial a_i\|\|_2$
1	S_I	0.5870e+06
2	S_G	0.1395e+05
3	p_2	0.4777e+04
4	G_0	0.3356e+01

Table 2.12: Glucose ranking with L_2 norm for MINMOD Millennium.

With these initial guesses, we performed a sensitivity analysis for MINMOD Millennium. The results are ranked in order in Table 2.12. Table 2.13 shows the typical normal values and normal ranges for glucose–insulin dynamics parameters in FSIGT. We can also confirm that all estimated parameters from our numerical simulation lie within their normal ranges.

Lipolysis model

In this subsection, we report on a semi–relative sensitivity analysis for the lipolysis model using data in [79]. The eight estimated parameters are S_G, S_I, c_x, l_0, l_2, X_2, m, and c_f. The meaning of each parameter is explained in Section 2.1.3. The initial guesses for these parameters were taken from [79],

	Typical normal	
Parameter	Value	Range
S_G	0.22e−01	(0.12e−02, 0.45e−01)
S_I	0.20e−03	(0.50e−04, 0.22e−02)
p_2	0.5e−01	(0.13e−02, 0.20)
G_0	200	(150, 400)
G_b	84	(65, 103)
I_b	10	(1, 32)

Table 2.13: Typical normal values and normal ranges for parameters [13].

and the estimated parameters are presented in Table 2.14. Table 2.15 gives

Parameter	S_G	S_I	c_x	l_0	l_2	X_2	m	c_f
Estimated	0.22077e−01	0.24383e−03	0.86664e−01	6.3474	16.849	13.035	3.2397	0.64721e−01
Initial	0.35063e−01	0.12000e−03	0.54091e−01	2.2481	42.856	11.259	1.8826	0.83893e−01

Table 2.14: Estimated parameters for the lipolysis model.
Relative l_2 error: 1.48e−02.

the results of the sensitivity analysis. As expected, we can observe that S_I and S_G are the two most sensitive parameters and infer that l_0, l_2, X_2, m, and c_f do not have any effect on the plasma glucose concentration. Also, performing a sensitivity analysis on the FFA states, we can observe that c_f and c_x are the two most sensitive parameters. These describe the first–order reaction rate for clearing FFA and the rate of influx and outflux for insulin in $X(t)$, respectively. In fact, c_x is designed to simulate the effects of insulin on the suppression of lipolysis and glucose disposal in the lipolysis model.

2.3 Numerical results

In this section, we present several numerical results for glucose–insulin dynamics. The numerical methods we have used are explained in Section 2.1.4

	Glucose states		FFA states	
Rank	Parameter a_i	$\|\|\partial G(t)/\partial a_i\|\|_2$	Parameter a_i	$\|\|\partial F(t)/\partial a_i\|\|_2$
1	S_I	0.1052e+07	c_f	0.2947e+05
2	S_G	0.6318e+04	c_x	0.6380e+04
3	c_x	0.8897e+03	l_0	0.1438e+03
4			X_2	0.7582e+02
5			m	0.7160e+02
6			l_2	0.5538e+02

Table 2.15: Glucose and FFA ranking with L_2 norm for the lipolysis model.

and Section 2.2. In Figure 2.2a, we have plotted the numerical results for several mathematical glucose–insulin models with their experimental data [76]. We can see that all of the numerical results fit the experimental data very well, except data for glucose in the early time. The relative l_2 errors for glucose concentration lie within 5.00e−02 in each model. For Arino's minimal model and MINMOD Millennium, we can observe that the glucose value converges to the baseline value (G_b), thus verifying the mathematical analysis in [25] and Section 2.1.2. The numerical results for $X(t)$ are shown in Figure 2.2b. We can observe that $X(t)$ takes non–negative values in all models. Mathematically, it has been proved that $X(t)$ always produces positive values in Arino's minimal model [25] and in MINMOD Millennium .

The computed insulin values are plotted in Figure 2.2c alongside their experimental values [76]. We can see that all of the numerical results fit the experimental data very well, except data for insulin in the early time. The relative l_2 errors for insulin concentration are within 9.00e−02 in each model. We can observe that the insulin values are greater than or equal to the baseline ($I_b = 7.3$) in Arino's model and the Arino–insulin kinetics model, but not in MINMOD or the MINMOD–insulin kinetics model. Mathematically, it has been proved that $I(t)$ always produces positive values and is greater than or

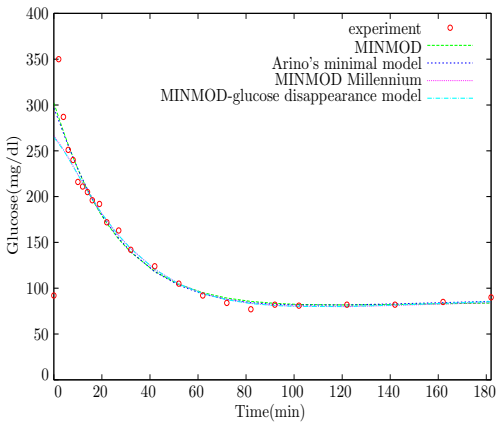

(a) Glucose dynamics.

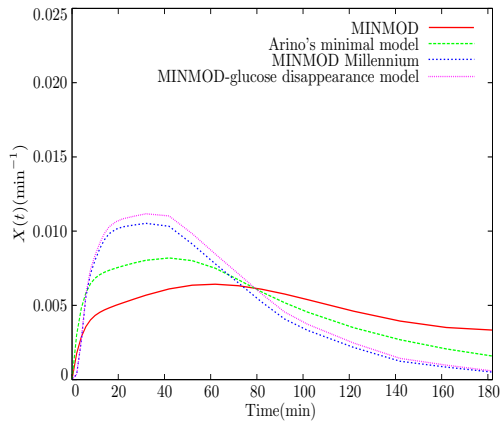

(b) Dynamics of $X(t)$.

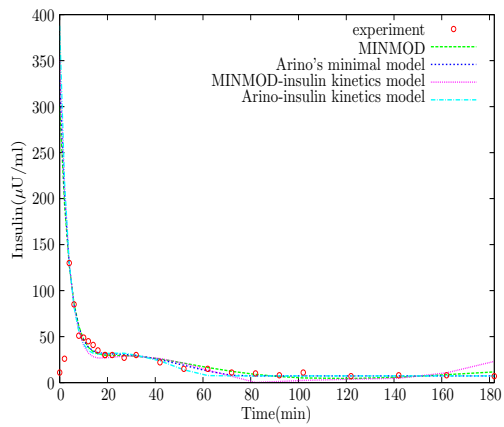

(c) Insulin dynamics.

Figure 2.2: Plot of experimental data and numerical results of each dynamics model.

equal to its baseline in Arino's model and the Arino–insulin kinetics model [25].

From the numerical results in Figure 2.2 and the mathematical analysis performed in [25] and Section 2.1.2, it is possible to conclude that Arino's minimal model is the best for understanding glucose–insulin dynamics. In reality, however, many researchers use MINMOD Millennium for their physiological purposes.

We have plotted the numerical results from the lipolysis model, which describes the FFA effect. In Figure 2.3a, the data for insulin, glucose, and FFA are plotted with the numerical results from the lipolysis model. The computed relative l_2 error is 1.48e−02. In Figure 2.3b, Figure 2.3c, and Figure 2.3d, we can confirm the limits of $G(t)$, $F(t)$, and $X(t)$ converge to their respective equilibrium points.

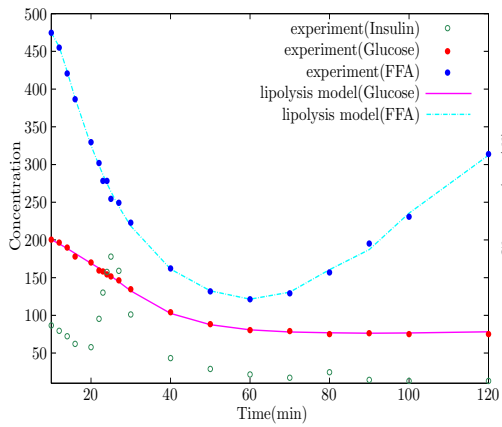

(a) Plots with experimental and computed values from the lipolysis model.

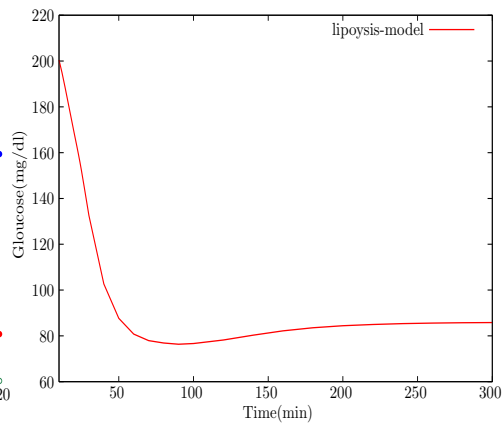

(b) Computed glucose in the lipolysis model.

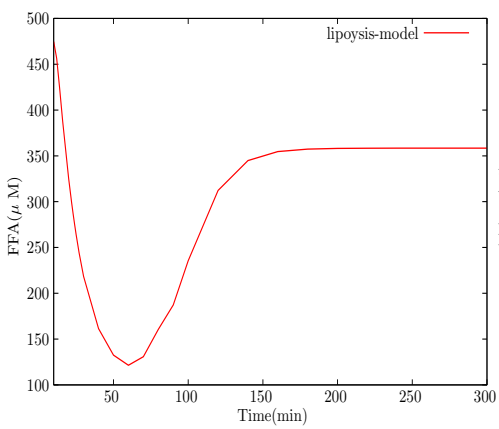

(c) Computed FFA in the lipolysis model.

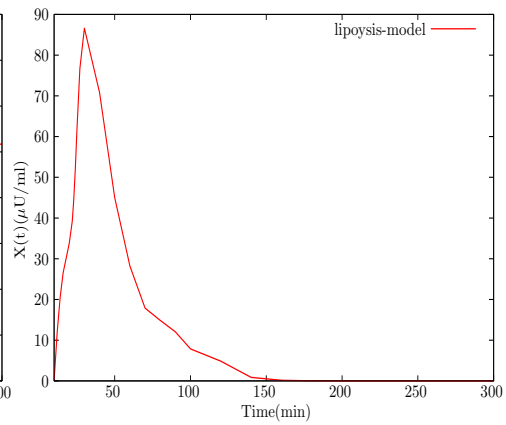

(d) Computed $X(t)$ in the lipolysis model.

Figure 2.3: Modeling results from the lipolysis model.

2.4 Conclusions

In Section 2.1, we proved that MINMOD Millennium and the lipolysis model have bounded and positive solutions under certain conditions. Also, we have showed that they have stable equilibrium points due to the homeostasis of insulin. In Section 2.2, using Levenberg–Marquardt parameter estimation and semi–relative sensitivity analysis [90], we estimated parameter values and found that S_I and γ are the most sensitive in the glucose–insulin system. In Section 2.3, we presented our numerical results for $G(t), X(t), I(t)$, and $F(t)$ with estimated parameters for each of the models discussed in Section 2.1, and verified that they are consistent with our analysis.

Chapter 3

A fractional–order model for MINMOD Millennium

3.1 The origin of the fractional calculus

Newton and Leibniz developed the notions of differentiation and integration of integer order. The symbol

$$\frac{d^n y}{dx^n}$$

invented by Leibniz denotes the nth derivative of a function y with respect to x. Differentiation and integration of noninteger order is originated from the letter between Leibniz and L'H$\hat{o}$pital in 1695 [55]. L'H$\hat{o}$pital asked Leibniz: "What does $\frac{d^n y}{dx^n}$ mean if n be $\frac{1}{2}$?" Leibniz replied: "It will lead to a paradox." But he added fatidically, "From this apparent paradox, one day useful consequences will be drawn." Leibniz [56] mentioned derivatives of "general order" in the

correspondence with Johann Bernoulli in 1695. In 1697, Leibniz [57] discussed Willis's infinite product for $\frac{\pi}{2}$ with him in the letter, Leibniz mentioned the notation $d^{1/2}y$ to achieve the same result for $\frac{\pi}{2}$. Euler was interested in the fractional calculus, and in 1730 he wrote: "When n is a positive integer, and if y is a function of x, the ratio $d^n y$ to dx^n can be expressed algebraically, so that if $n = 2$ and $y = x^3$, then d^2x^3 to dx^2 is $6x$ to 1. Now it is asked what kind of ratio can then be made if n be a fraction. The difficulty in this case can easily be understood. For if n is a positive integer d^n can be found by continued differentiation. Such a way, however, is no evident if n is a fraction. But yet with the help of interpolation which I have already explained in this dissertation, one may be able to expedite the matter [39]." In 1819, the French mathematician Lacroix [52] firstly mentioned a derivative of arbitrary order in his text. He developed nth derivative of $y = x^m$, for a positive integer m,

$$\frac{d^n y}{dx^n} = \frac{m!}{(m-n)!} x^{m-n},$$

where $n\ (\leq m)$ is an integer. By using the gamma function $\Gamma(x) = \int_0^\infty t^{x-1} e^{-t} dt$, he got the formula for the fractional derivative

$$\frac{d^\alpha y}{dx^\alpha} = \frac{\Gamma(\beta+1)}{\Gamma(\beta-\alpha+1)} x^{\beta-\alpha},$$

where α and β are fractional numbers. He then calculated the example for $y = x$ and $\alpha = 1/2$,

$$\frac{d^{1/2} y}{dx^{1/2}} = \frac{2\sqrt{x}}{\sqrt{\pi}}.$$

In 1822, Fourier [42] easily obtained an integral representations for $f(x)$

and its derivatives:

$$f(x) = \frac{1}{2\pi} \int_{-\infty}^{\infty} f(\xi) d\xi \int_{-\infty}^{\infty} \cos p(x - \xi)\, dp,$$

and

$$\frac{d^n}{dx^n} f(x) = \frac{1}{2\pi} \int_{-\infty}^{\infty} f(\xi) d\xi \int_{-\infty}^{\infty} p^n \cos\{p(x - \xi) + \frac{1}{2} n\pi\}\, dp$$

for an integer n.

Replacing integer n with any real number α, he had the fractional operation from integral representation of $f(x)$:

$$\frac{d^\alpha}{dx^\alpha} f(x) = \frac{1}{2\pi} \int_{-\infty}^{\infty} f(\xi) d\xi \int_{-\infty}^{\infty} p^\alpha \cos\{p(x - \xi) + \frac{1}{2} \alpha\pi\}\, dp.$$

Fourier mentioned: "The number α that appears in the above will be regarded as any quantity whatsoever, positive or negative."

The first application of fractional operations was made by Abel in 1823 [1]. He applied the fractional calculus in the solution of an integral equation based on the tautochronous problem. The solution is originated from the fact that the derivative of a constant function is not always equal to zero.

Augustus De Morgan mentioned about fractional calculus: "Both these system may very possibly be parts of a more general system, but at present I incline to the conclusion that neither system has any claim to be considered as giving the form $\frac{d^n}{dx^n} x^m$, though either may be a form [26]." The doubtful point noted by Morgan is now solved.

After that, many famous mathematicians have devoted their energies to fractional calculus over the years, and some definitions of fractional derivative have been contributed [46, 65, 80]. Among them, we introduce several well–known definitions by Riemann–Liouville, Caputo, and Grünwald.

Riemann [59] devoted his posthumous published *Gesammelte Werke* (1892) to fractional integration. He found a generalized Taylor series and derived the following definition for fractional integration:

$$J_c^\alpha f(x) = \frac{1}{\Gamma(\alpha)} \int_c^x (x-k)^{\alpha-1} f(k)\, dk + \phi(x). \tag{3.1}$$

In order to definitize the lower limit of integration c, he added a complementary function $\phi(x)$.

The Riemann–Liouville definition appeared in the paper written by Sonin (1869) [91]. By using a contour integration on the Riemann surface, the definition is given by

$$J_c^\alpha f(x) = \frac{1}{\Gamma(\alpha)} \int_c^x (x-k)^{\alpha-1} f(k)\, dk, \quad Re\, \alpha > 0, \tag{3.2}$$

for integration of an arbitrary order α.

If $x > c$ in the definition (3.2), we obtain the definition (3.1) without a complementary function $\phi(x)$. When $c = 0$ in (3.2), we have

$$J_0^\alpha f(x) = \frac{1}{\Gamma(\alpha)} \int_0^x (x-k)^{\alpha-1} f(k)\, dk, \quad Re\, \alpha > 0. \tag{3.3}$$

This form is often considered to be the Riemann–Liouville fractional integral.

By using the Riemann–Liouville fractional integral (3.3), one can define the Riemann–Liouville fractional derivative of f with order α given by

$${}_{RL}D_0^\alpha f(x) = \frac{d^{\lceil \alpha \rceil}}{dx^{\lceil \alpha \rceil}} J_0^{\lceil \alpha \rceil - \alpha} f(x), \quad \alpha > 0, \tag{3.4}$$

where $\lceil . \rceil$ is the ceiling function.

Caputo introduced a definition of fractional derivative which has an alternative form of the Riemann–Liouville fractional derivative (3.4). This is

defined by

$$ {}_C D_0^{\alpha} f(x) = J_0^{\lceil \alpha \rceil - \alpha} \frac{d^{\lceil \alpha \rceil}}{dx^{\lceil \alpha \rceil}} f(x), \quad \alpha > 0. \tag{3.5} $$

Grünwald developed a definition for fractional derivative as the limit of a sum. It is defined by

$$ \frac{d^{\alpha}}{dx^{\alpha}} f(x) = \lim_{h \to 0} \frac{1}{h^{\alpha}} \sum_{k=0}^{m} (-1)^k \frac{\Gamma(\alpha + 1) f(x - kh)}{\Gamma(k+1)\Gamma(\alpha - k + 1)}, \tag{3.6} $$

provided the limit exists.

By using the identity $(-1)^k \dfrac{\Gamma(\alpha+1)}{\Gamma(\alpha - k + 1)} = \dfrac{\Gamma(k - \alpha)}{\Gamma(-\alpha)}$, the definition (3.6) is replaced by

$$ \frac{d^{\alpha}}{dx^{\alpha}} f(x) = \lim_{h \to 0} \frac{h^{-\alpha}}{\Gamma(-\alpha)} \sum_{k=0}^{m} \frac{\Gamma(k - \alpha)}{\Gamma(k+1)} f(x - kh). \tag{3.7} $$

If α in (3.7) is equal to an integer n, then we have

$$ \frac{d^n}{dx^n} f(x) = \lim_{h \to 0} \frac{1}{h^n} \sum_{k=0}^{m} (-1)^k \binom{n}{k} f(x - kh), \tag{3.8} $$

where $\binom{n}{k}$ is the binomial coefficient.

The classical definitions $\dfrac{d}{dx} f(x)$, $\dfrac{d^2}{dx^2} f(x) \cdots$, $\dfrac{d^n}{dx^n} f(x)$ lead to the result (3.8).

In recent years, the fractional derivative have been extensively considered in many fields. We will discuss its applications for various fields in the next section.

3.2 Motivation

The glucose–insulin mechanism has been mathematically modeled and studied by many researchers [4–7, 12–14, 25, 28, 36, 43, 62, 69, 76, 79, 85, 86, 97, 98]. We compared and analyzed several models in Chapter 2. Among many valuable works, Bergman *et al.* [7] proposed a three–compartment minimal model to analyze and estimate insulin sensitivity and pancreatic responsivity to determine glucose tolerance. In 1986, Pacini and Bergman [76] applied the model to MINMOD, which is a computer program for the identification of model parameters for each individual. Since then, modified versions of the minimal model have been introduced by a number of researchers [5, 13, 25, 28, 79].

In particular, in 2003, Boston *et al.* [13] developed a new program, MINMOD Millennium, which provides estimates of insulin sensitivity and glucose effectiveness for almost every subject in contrast to earlier MINMOD versions and some other minimal model programs. It is extensively used to study the glucose–insulin systems by many physiologists and researchers [53, 82, 87, 93]. Rudic *et al.* [87] examined the role of the molecular clock in glucose homeostasis by using MINMOD Millennium. Larson–Meyer *et al.* [53] used the program to confirm that large adipocytes cause lipids to be deposited in visceral and hepatic tissues, promoting insulin resistance. Srinivasan *et al.* [93] applied MINMOD Millennium to analyze the effect of metformin treatment on insulin sensitivity, and Punjabi *et al.* [82] used it to find that sleep–disordered breathing is intimately related to impairment in insulin sensitivity, glucose effectiveness, and pancreatic β-cell functions independent of adiposity. Figure 3.1 shows such input–output procedures to estimate parameter with MINMOD Millennium.

However, a number of models have been restricted to integer–order ordinary (or delay) differential equations. Recently, fractional calculus has been

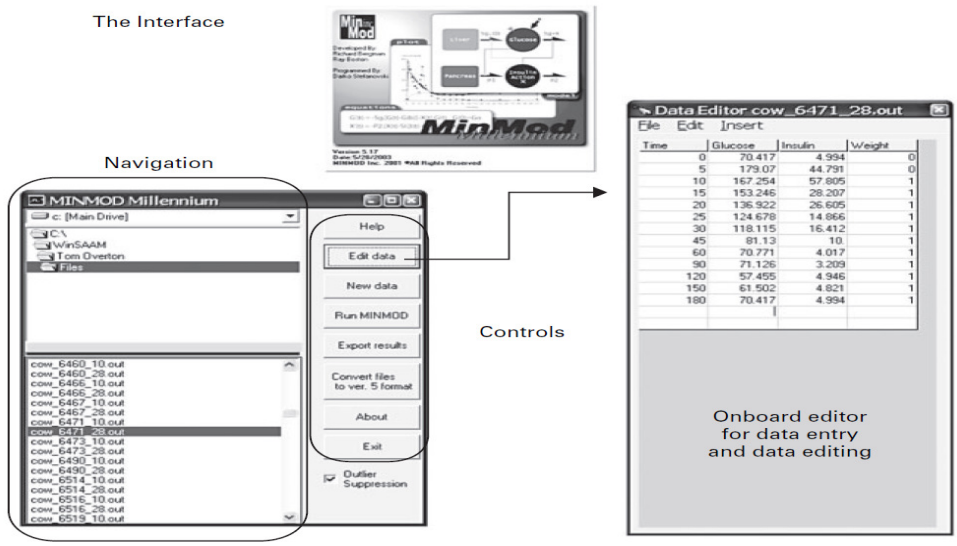

Figure 3.1: Input–output from the user–friendly program MINMOD Millennium (copyright R.N. Bergman) [5].

widely applied in many fields [2, 9, 17, 22, 35, 37, 44, 64, 70, 73, 74, 81, 101], and it has been shown that the modeling of fractional ordinary differential equations has a number of advantages over classical integer–order ones. Many mathematicians and researchers have tried to model real–world problems using fractional calculus. In control theory, fractional–order dynamical systems are an effective method for time–domain analysis problems. Podlubny [81] introduced $PI^{\lambda}D^{\mu}$-controller which is a new type of a fractional–order controller and also showed it has better performance than the classical PID-controller. Oustaloup [74] developed CRONE–controller (Commande Robuste d'Ordre Non Entrier controller) using fractional derivative. Nigmatullin and Nelson [70] used fractional–order to develop fractional kinetics in complex systems. Le Mehaute and Crepy [64] applied fractance, which represents an electrical element with fractional–order impedance, to electrical circuits. Westerlund

[101] generalized voltage divider in the fractional–order impedances. In electromagnetism, Engheta [37] extended the integer–order multiples related to powers of 2 to the fractional–order 2^{α}. Scott Blair [9], Gerasimov [44], Caputo and Mainardi [17] proposed fractional–order laws of deformation for modeling the viscoelastic behavior of real materials. Oldham and Spanier [73] used the fractional–order integral law to suggest the replacement of the classical integer–order Fick's law describing the diffusion of electroactive species toward the electrodes. In biology, Anastasio [2] suggested that fractional-order dynamics could describe pre-motor neurons and motoneurons, and Cole [22] used fractional-order electric conductance to represent the cell membranes of biological organisms. Djordjević *et al.* [35] confirmed that fractional derivatives embody some essential features in the rheological behavior of biological cells.

Numerous researchers have studied the relationship of blood rheology to glucose–insulin [24, 61, 67, 78]. Perez–Martin *et al.* [78] found that plasma viscosity is a marker of insulin resistance in patients, and Coppola *et al.* [24] evaluated the effect of insulin on blood rheology in non–diabetic subjects and in patients with type 2 diabetes. MacRury and Lowe [61] confirmed that some abnormalities can be found in the blood viscosity of patients with diabetes mellitus. Moan *et al.* [67] found statistically negative correlations between the glucose disposal rate (GDR) and calculated whole–blood viscosity at both high and low shear rates.

Hence, we propose a system of fractional–order differential equations for modeling the glucose–insulin dynamics. In this chapter, we introduce a model that contains fractional–order differential equations of order $0 < \alpha \leq 1$ into MINMOD Millennium. Section 3.3 is devoted to the derivation and analysis of the fractional–order system in MINMOD Millennium. In Section 3.4, we

describe the numerical method, including how to determine the optimal initial guess for the new model. The optimal fractional order and parameters are estimated for many experimental data (normal subjects and type 2 diabetic patients) in Section 3.5. From these results, we not only confirm that our analysis is correct, but also verify that the insulin sensitivity (S_I) in diabetics is significantly lower than in non–diabetics. Moreover, we find the new factor ($\tau^{1-\alpha}$) determining glucose tolerance and the relation between S_I and $\tau^{1-\alpha}$.

3.3 Model derivation

There are several definitions for fractional derivatives and integrals. Here and throughout, we will adopt Caputo's definition of fractional–order differentiation, as this has some advantages for initial–value problems.

Recall Euler's Gamma function (or Euler's integral of the second kind) as follows:

$$\Gamma(x) = \int_0^\infty t^{x-1} e^{-t} dt. \tag{3.9}$$

We then begin by clarifying the definitions of fractional–order integration and differentiation; see, for instance, [46].

Denote by $\mathbb{R}_+$ and $\mathbb{R}_+^n$ the set of strictly positive real numbers and set of points with positive components in $\mathbb{R}^n$, respectively.

Definition 3.3.1. *Let $\alpha \in \mathbb{R}_+$. The function $J_a^\alpha f(t)$, defined by*

$$J_a^\alpha f(t) = \frac{1}{\Gamma(\alpha)} \int_a^t (t-u)^{\alpha-1} f(u) du, \tag{3.10}$$

is called the Riemann–Liouville fractional integral of order α.

Definition 3.3.2. *Let $\alpha \in \mathbb{R}_+$ and $m = \lceil \alpha \rceil$. Then, the Caputo fractional*

derivative of order α *is defined as the function* ${}_C D_a^\alpha f(t)$ *given by*

$$ {}_C D_a^\alpha f(t) = J_a^{m-\alpha} D^m f(t), \tag{3.11}$$

where $\lceil . \rceil$ *is the ceiling function such that* $\lceil x \rceil = \min\{z \in \mathbb{Z} : z \geq x\}$, *and* $D^m = \frac{d^m}{dt^m}$.

The Laplace transform of Caputo fractional derivative (3.11) is given as follows:

$$\mathcal{L}({}_C D_a^\alpha f(t)) = \int_0^\infty {}_C D_a^\alpha f(t) e^{-st} dt = s^\alpha \mathcal{L}(f(t)) - s^{\alpha-1} f(0), \quad 0 < \alpha \leq 1. \tag{3.12}$$

Let us introduce a generalized MINMOD Millennium model by using fractional-order differentiation of order $\alpha \in (0, 1]$ in the following form:

$$ {}_C D_0^\alpha G(t) = -({S_G}^\alpha + \tau^{1-\alpha} X(t)) G(t) + {S_G}^\alpha G_b, \quad G(0) = G_0, \tag{3.13a}$$

$$ {}_C D_0^\alpha X(t) = -{p_2}^\alpha (X(t) - S_I (I(t) - I_b)^+), \quad X(0) = 0, \tag{3.13b}$$

$$(I(t) - I_b)^+ = \begin{cases} I(t) - I_b & I(t) \geq I_b, \\ 0 & I(t) < I_b, \end{cases}$$

where the nomenclature is as follows:

$G(t)$ $[mg/dl]$:	the plasma glucose concentration at time t $[min]$;
$I(t)$ $[\mu U/ml]$:	the plasma insulin concentration at time t $[min]$;
G_b $[mg/dl]$:	the basal glucose value;
I_b $[\mu U/ml]$:	the basal insulin value;
$X(t)$ $[min^{-1}]$:	the insulin action in proportion to interstitial insulin;
S_G $[min^{-1}]$:	the glucose effectiveness;
p_2 $[min^{-1}]$:	a parameter describing the removal rate of insulin from the interstitial space;
S_I $[min^{-1}(\mu U/ml)^{-1}]$:	the insulin sensitivity;
G_0 $[mg/dl]$:	the initial plasma glucose concentration;
τ $[min]$:	a time constant needed to preserve units.

Remark 3.3.3. *In* (3.13a)*, $\tau^{1-\alpha}$ can be considered as the effect of the rheological behavior in increasing the muscular and liver sensibility to the action of insulin [6, 7, 28] in physiology. This means that the more the decrease of insulin sensitivity (S_I), the more the need of the active rate ($\tau^{1-\alpha}$) to maintain the balance of glucose–insulin.*

Remark 3.3.4. *$I(t)$ is an input variable while $G(t)$ and $X(t)$ are output variables in* (3.13)*. In this system, $G(t)$ and $I(t)$ affect each other physiologically which behaves in a nonlinear fashion. Moreover, $I(t)$ is considered as bounded and piecewise C^1 function.*

For the notational convenience, denote $C^1(\mathbb{R}_+, \mathbb{R}^2)$ by the Banach space of continuously differentiable functions mapping $\mathbb{R}_+$ into $\mathbb{R}^2$, $\mathbf{x}(t)$ by $\mathbf{x}(t) = (x_1(t), x_2(t))^T = (G(t), X(t))^T \in C^1(\mathbb{R}_+, \mathbb{R}^2)$, and the right hand side in (3.13)

by

$$\mathbf{f}(t,\mathbf{x};\mathbf{a}) = -\begin{pmatrix} {S_G}^{\alpha} x_1(t) + \tau^{1-\alpha} x_1(t) x_2(t) \\ {p_2}^{\alpha} x_2(t) \end{pmatrix} + \begin{pmatrix} {S_G}^{\alpha} G_b \\ p_2^{\alpha} S_I (I(t) - I_b)^{+} \end{pmatrix}, \quad (3.14)$$

where $\mathbf{a} = \{S_G, p_2, S_I, G_0, I_0, \alpha\}$ is a set of parameters. Then (3.13) can be rewritten as

$$ {}_C D_0^{\alpha} \mathbf{x}(t) = \mathbf{f}(t,\mathbf{x};\mathbf{a}), \quad \mathbf{x}(0) = \begin{pmatrix} G_0 \\ 0 \end{pmatrix}. \quad (3.15)$$

In particular, when the input $I(t) = 0$, the system is called the homogeneous system of (3.15). Let us denote by $||\cdot||$, the discrete l_2 norm and by $spec(\mathbf{A})$, the eigenvalues of matrix $\mathbf{A}$. These notations will be used throughout this section.

To discuss the non–negativity and boundedness of the solution of (3.15), the following preliminaries are needed.

Theorem 3.3.5. (Theorem 2.1., Remark 2.3., and Theorem 3.1. in [60]) *Consider the following initial value problem for Caputo fractional differential equations*

$$\begin{cases} {}_C D_{t_0}^{\alpha} \mathbf{x} = \mathbf{f}(t,\mathbf{x}), \quad 0 < \alpha \leq 1, \\ \mathbf{x}(t_0) = \mathbf{x}_0, \end{cases} \quad (3.16)$$

where the function $\mathbf{f}(t,\mathbf{x}) : \mathbb{R} \times \mathbb{R}^d \to \mathbb{R}^d$ *is a vector field and the dimension* $d \geq 1$. *Choose any* $a, b \in \mathbb{R}_+$, *and let*

$$\begin{aligned} \mathcal{T} =& [t_0 - a, t_0 + a], \quad \mathcal{B} = \{\mathbf{x} \in \mathbb{R}^d | \, ||\mathbf{x} - \mathbf{x}_0|| \leq b\}, \\ \mathcal{D} =& \{(t,\mathbf{x}) \in \mathbb{R} \times \mathbb{R}^d \,|\, t \in \mathcal{T}, \mathbf{x} \in \mathcal{B}\}. \end{aligned}$$

Assume that the function $\mathbf{f}(t,\mathbf{x}) : \mathcal{D} \to \mathbb{R}^d$ *satisfies the following conditions:*

1. $\mathbf{f}(t, \mathbf{x})$ *is Lebesgue measurable with respect to* t *on* $\mathcal{T}$*;*

2. $\mathbf{f}(t, \mathbf{x})$ *is continuous with respect to* $\mathbf{x}$ *on* $\mathcal{B}$*;*

3. *there exists a bounded real–valued function* $M(t)$ *such that*

$$||\mathbf{f}(t, \mathbf{x})|| \leq M(t),$$

for almost every $t \in \mathcal{T}$ *and all* $\mathbf{x} \in \mathcal{B}$*.*

Then, there at least exists a solution of the initial value problem (3.16) *on the interval* $[t_0 - h, t_0 + h]$ *for some positive number* h *satisfying*

$$\mathbf{x}(t) = \mathbf{x}_0 + J_{t_0}^{\alpha} \left(\mathbf{f}(t, \mathbf{x}) \right).$$

Moreover, if the vector field $\mathbf{f}(t, \mathbf{x})$ *satisfies the above first two conditions 1 and 2 in the global space* $\mathbb{R} \times \mathbb{R}^d$ *and*

$$||\mathbf{f}(t, \mathbf{x})|| \leq \lambda ||\mathbf{x}|| + w, \tag{3.17}$$

for almost every $t \in \mathbb{R}$ *and all* $\mathbf{x} \in \mathbb{R}^d$ *where* λ, w *are two positive constants, then, there exists a function* $\mathbf{x}(t)$ *on* $(-\infty, \infty)$ *satisfying the initial condition in* (3.16)*. If* $\nabla_{\mathbf{x}} \mathbf{f}(t, \mathbf{x})$ *is further assumed to be continuous with respect to* $\mathbf{x}$*, this gives the uniqueness of the solution* $\mathbf{x}(t)$ *in* (3.16)*.*

Lemma 3.3.6. (Generalized Mean Value Theorem in [72])

Let $0 < \alpha \leq 1$*. Suppose that* $f \in C[a, b]$ *and* ${}_C D_a^{\alpha} f \in C(a, b]$*. Then, for all* $t \in (a, b]$*, there exist* $\xi \in (a, t)$ *such that*

$$f(t) = f(a) + \frac{1}{\Gamma(\alpha)} ({}_C D_a^{\alpha} f)(\xi)(t - a)^{\alpha}. \tag{3.18}$$

Corollary 3.3.7. (Corollary 1. in [34]) *Let* $0 < \alpha \leq 1$. *Suppose that* $f \in C[a,b]$ *and* ${}_C D_a^{\alpha} f \in C(a,b]$. *If* ${}_C D_a^{\alpha} f(t) \geq 0,\ \forall t \in (a,b)$, *then* f *is a non–decreasing function. If* ${}_C D_a^{\alpha} f(t) \leq 0, \forall t \in (a,b)$, *then* f *is a non–increasing function.*

Lemma 3.3.8. (Fractional Comparison Principle in [58])

Let $x(0) = y(0)$ *and* ${}_C D_0^{\alpha} x(t) \leq {}_C D_0^{\alpha} y(t)$, *where* $0 < \alpha \leq 1$. *Then* $x(t) \leq y(t)$.

Definition 3.3.9. *For Re* $\alpha > 0$, *the Mittag–Leffler function* E_α *is defined by*

$$E_\alpha(z) := \sum_{j=0}^{\infty} \frac{z^j}{\Gamma(j\alpha + 1)}. \tag{3.19}$$

Moreover, it is an entire function if $\alpha > 0$.

The Mittag–Leffler function with two parameters defined by

$$E_{\alpha,\beta}(z) := \sum_{j=0}^{\infty} \frac{z^j}{\Gamma(j\alpha + \beta)} \tag{3.20}$$

is an entire function whenever $\alpha > 0, \beta > 0$ and $z \in \mathbb{C}$. The Laplace transform of the Mittag–Leffler function with two parameters is given by

$$\mathcal{L}(t^{\beta-1} E_{\alpha,\beta}(-\lambda t^{\alpha})) = \frac{s^{\alpha-\beta}}{s^{\alpha} + \lambda}, \quad Re(s) > |\lambda|^{1/\alpha}. \tag{3.21}$$

The following lemmas are useful in the proof of the non–negativity, boundedness, and stability of the solution (3.15).

Lemma 3.3.10. (Page 210 in [38]) *Suppose that* $0 < \alpha < 2$, $\beta \in \mathbb{R}$, *and* $\mu \in \left(\frac{\alpha\pi}{2}, min\{\pi, \alpha\pi\}\right)$. *Then for an arbitrary integer* $N \geq 1$, *the following asymptotic expansion holds:*

$$E_{\alpha,\beta}(z) = -\sum_{j=1}^{N} \frac{1}{\Gamma(-j\alpha+\beta)} \frac{1}{z^j} + \mathcal{O}\left(\frac{1}{z^{N+1}}\right), \text{ as } |z| \to \infty, \ \mu \leq |arg(z)| \leq \pi. \tag{3.22}$$

Lemma 3.3.11. (Theorem 1.6. in [80]) *Suppose that* $0 < \alpha < 2$, $\beta \in \mathbb{R}$, *and* $\mu \in \left(\frac{\alpha\pi}{2}, min\{\pi, \alpha\pi\}\right)$. *Then there exists* $M > 0$ *such that*

$$|E_{\alpha,\beta}(z)| \leq \frac{M}{1+|z|}, \quad \mu \leq |arg(z)| \leq \pi. \tag{3.23}$$

Lemma 3.3.12. (Corollary 1. in [100]) *Suppose that* $\mathbf{A} \in \mathbb{C}^{n\times n}$, $0 < \alpha < 2$, $\beta \in \mathbb{R}$, *and* $\mu \in \left(\frac{\alpha\pi}{2}, min\{\pi, \alpha\pi\}\right)$. *Then there exists* $C > 0$ *such that*

$$||E_{\alpha,\beta}(\mathbf{A})|| \leq \frac{C}{1+||\mathbf{A}||}, \tag{3.24}$$

where $\mu \leq |arg(spec(\mathbf{A}))| \leq \pi$.

By the help of Lemmas, we now prove the existence of the solution in (3.15).

Proposition 3.3.13. *There is a solution* $\mathbf{x}(t)$ *in* (3.15) *that remains in* $\mathbb{R}^2_+$. *We also have*

$$\limsup_{t\to\infty} \ x_1(t) \leq G_b. \tag{3.25}$$

Proof. $\mathbf{f}(t, \mathbf{x}; \mathbf{a})$ in (3.15) satisfies clearly the conditions 1 and 2 of Theorem 3.3.5 in $\mathbb{R}_+ \cup \{0\} \times \mathbb{R}^2$.

We now show that it satisfies the condition (3.17).

Due to the boundedness for $I(t)$, ${}_C D_0^\alpha x_2(t)$ in (3.15) satisfies

$$||{}_C D_0^\alpha x_2(t)|| \leq p_2^\alpha ||x_2(t)|| + p_2^\alpha S_I M, \tag{3.26}$$

where $M = \sup_{t\geq 0} ||I(t) - I_b||$.

Then, Theorem 3.3.5 gives the existence and uniqueness of solution $x_2(t)$ on $(0, \infty)$.

In addition, we have

$$\begin{aligned} {}_C D_0^{\alpha} x_2(t) &\leq -{p_2}^{\alpha} x_2(t) + p_2^{\alpha} S_I M \\ &= -{p_2}^{\alpha} \left(x_2(t) - S_I M \right). \end{aligned} \tag{3.27}$$

Let $K(t) = x_2(t) - S_I M$. Then, using the the linearity of Caputo derivative, (3.27) can be rewritten as follows:

$$ {}_C D_0^{\alpha} K(t) \leq -{p_2}^{\alpha} K(t),$$

By applying Lemma 3.3.8, we have

$$K(t) \leq K(0) E_{\alpha,1}(-{p_2}^{\alpha} t^{\alpha}) \quad \forall t > 0, \tag{3.28}$$

and thus we have $\limsup_{t\to\infty} x_2(t) \leq S_I M$, by Lemma 3.3.11, and it follows that there exists a constant $R > 0$ such that $||x_2(t)|| \leq R$.

${}_C D_0^{\alpha} x_1(t)$ in (3.15) satisfies

$$\begin{aligned} ||{}_C D_0^{\alpha} x_1(t)|| &\leq ||{S_G}^{\alpha} + \tau^{1-\alpha} x_2(t)||\ ||x_1(t)|| + {S_G}^{\alpha} G_b \\ &\leq \left({S_G}^{\alpha} + \tau^{1-\alpha} R \right) ||x_1(t)|| + {S_G}^{\alpha} G_b, \end{aligned} \tag{3.29}$$

which gives the sufficient condition for global existence and uniqueness of solution $x_1(t)$ in Theorem 3.3.5.

Therefore, the existing solution for (3.15) is

$$\mathbf{x}(t) = \mathbf{x}(0) + J_0^{\alpha} \left(\mathbf{f}(t, \mathbf{x}; \mathbf{a}) \right). \tag{3.30}$$

The non–negativity of the solution follows from

$$ {}_C D_0^{\alpha} \mathbf{x}(t) \mid_{\mathbf{x}(t)=0} = \begin{pmatrix} {S_G}^{\alpha} G_b \\ {p_2}^{\alpha} S_I (I(t) - I_b)^+ \end{pmatrix} \geq \begin{pmatrix} 0 \\ 0 \end{pmatrix}, \tag{3.31} $$

and Corollary 3.3.7. Thus the solution remains in $\mathbb{R}^2_+$.

From (3.15), we have

$$ {}_C D_0^{\alpha} x_1(t) \leq -{S_G}^{\alpha} x_1(t) + {S_G}^{\alpha} G_b. \tag{3.32} $$

Let $L(t) = x_1(t) - G_b$. (3.32) gives

$$ {}_C D_0^{\alpha} L(t) \leq -{S_G}^{\alpha} L(t), $$

By Lemma 3.3.8, we get

$$ L(t) \leq L(0) E_{\alpha,1}(-{S_G}^{\alpha} t^{\alpha}) \quad \forall t > 0. \tag{3.33} $$

Therefore, we have $\limsup_{t \to \infty} x_1(t) \leq G_b$, by Lemma 3.3.11. This proves (3.25). Thus the proof is completed. □

In addition to the existence of solution, we are going to prove the stability of fractional–order system with $\alpha \in (0, 1)$ in (3.15). In order to analyze the stability of the fractional–order model, we quote the following lemmas.

Lemma 3.3.14. (The proof of Theorem 4.1.(a) in [83]) *For any $t \geq 0$ and $\alpha \in (0, 1)$, suppose that all the eigenvalues of matrix $\mathbf{A} = (a_{ij})_{n \times n} \in \mathbb{R}^{n \times n}$ satisfy $|arg(spec(\mathbf{A}))| > \dfrac{\alpha \pi}{2}$. Then, there exists a positive constant N such that*

$$ \int_0^t ||\theta^{\alpha - 1} E_{\alpha,\alpha}(\theta^{\alpha} \mathbf{A})|| d\theta \leq N. \tag{3.34} $$

Lemma 3.3.15. (Gronwall's lemma in [49])

Let $x(t)$ and $f(t)$ be real–valued piecewise continuous functions defined on the real interval $[a, b]$, let $z(t) \in L(a, b)$ be also real–valued, and $x(t)$ and $z(t)$ are nonnegative on the interval. If

$$x(t) \leq f(t) + \int_a^t z(\tau)x(\tau)d\tau \tag{3.35}$$

then, we have

$$x(t) \leq f(t) + \int_a^t f(\tau)z(\tau)exp\Big\{\int_\tau^t z(s)ds\Big\}d\tau, \quad \forall\ t \in [a, b]. \tag{3.36}$$

Recall that experimental results [7, 8, 25, 50, 66, 77, 79, 84, 99] suggest that $I(t)$ reaches a steady state (I_∞), which is in a neighborhood of I_b, due to the homeostasis of insulin. Thus given $\epsilon > 0$, it is reasonable to consider a time $t^*(\epsilon)$ such that $|I(t) - I_\infty| < \epsilon$ if $t \geq t^*(\epsilon)$. Then one may seek a steady state solution of (3.15) in such a neighborhood.

Indeed, we have the following proposition.

Proposition 3.3.16. *Assume that for every $\epsilon > 0$, there exists $t^*(\epsilon)$ such that $|I(t) - I_\infty| < \epsilon$ for all $t \geq t^*(\epsilon)$. Then, $\mathbf{x}(t) = (x_1(t), x_2(t))^T$ of the system* (3.15) *has a stable equilibrium point $(G_b, 0)^T$, which is also a stable equilibrium point of the homogeneous system.*

Proof. By recalling the homogeneous system of (3.15), we can compute the equilibrium point ($\mathbf{x}_{eq}$) of the system which has an explicit form of

$$\mathbf{x}_{eq} = \begin{pmatrix} G_b \\ 0 \end{pmatrix}.$$

The change of variables $\widetilde{\mathbf{x}}(t) = \mathbf{x}(t) - \mathbf{x}_{eq}$, transforms the homogeneous system

to

$$ {}_CD_0^{\alpha}\widetilde{\mathbf{x}}(t) = -\begin{pmatrix} {S_G}^{\alpha}\widetilde{x}_1(t) + \tau^{1-\alpha}(\widetilde{x}_1(t) + G_b)\widetilde{x}_2(t) \\ {p_2}^{\alpha}\widetilde{x}_2(t) \end{pmatrix}, \ \widetilde{\mathbf{x}}(t) = \begin{pmatrix} \widetilde{x}_1(t) \\ \widetilde{x}_2(t) \end{pmatrix}. \tag{3.37} $$

The linearized system of (3.37) at the zero equilibrium point is

$$ {}_CD_0^{\alpha}\widetilde{\mathbf{x}}(t) = \mathbf{A}(\mathbf{a})\widetilde{\mathbf{x}}(t) + \mathbf{h}(\widetilde{\mathbf{x}}(t); \mathbf{a}), \tag{3.38} $$

where the Jacobian matrix $\mathbf{A}(\mathbf{a})$ and the nonlinear part $\mathbf{h}(\widetilde{\mathbf{x}}(t); \mathbf{a})$ are given by

$$ A(\mathbf{a}) = \begin{pmatrix} -{S_G}^{\alpha} & -\tau^{1-\alpha}G_b \\ 0 & -{p_2}^{\alpha} \end{pmatrix}, \quad \mathbf{h}(\widetilde{\mathbf{x}}(t); \mathbf{a}) = \begin{pmatrix} -\tau^{1-\alpha}\widetilde{x}_1(t)\widetilde{x}_2(t) \\ 0 \end{pmatrix}. $$

Since $spec(\mathbf{A}(\mathbf{a})) = \{-{S_G}^{\alpha}, -{p_2}^{\alpha}\}$, we have $|arg(spec(\mathbf{A}(\mathbf{a})))| > \dfrac{\alpha\pi}{2}$.

In order to analyze the stability, we consider the dynamics of solution $\widetilde{\mathbf{x}}(t)$ after certain time. To determine the proper time, we choose $t^{**}(\epsilon)$ in addition to $t^{*}(\epsilon)$ which is already specified in the assumption.

For any ϵ, there exists $t^{**}(\epsilon)$ such that

$$ \frac{1}{1 + ||\mathbf{A}(\mathbf{a})||t^{\alpha}} < \epsilon \tag{3.39} $$

for all $t \geq t^{**}(\epsilon)$.

By using the assumption and (3.39), the time T can be chosen as the maximum between t^{*} and t^{**}, and we consider the system (3.15) with initial condition $\widetilde{\mathbf{x}}(T) = (\widetilde{x}_1(T), \widetilde{x}_2(T))^T$ which is bounded.

We split the system (3.15) with initial time T into the linear and nonlinear part which is

$$ {}_CD_0^{\alpha}\widetilde{\mathbf{x}}(t+T) = \mathbf{A}(\mathbf{a})\widetilde{\mathbf{x}}(t+T) + \mathbf{h}(\widetilde{\mathbf{x}}(t+T); \mathbf{a}) + \mathbf{g}(t+T; \mathbf{a}), \tag{3.40} $$

where $\mathbf{g}(t+T;\mathbf{a})$ with the input function $I(t)$ is given by

$$\mathbf{g}(t+T;\mathbf{a}) = \begin{pmatrix} 0 \\ p_2^{\alpha} S_I (I(t+T) - I_b)^{+} \end{pmatrix}.$$

Denote $\widetilde{\mathbf{X}}(s)$ by the Laplace transform of $\widetilde{\mathbf{x}}(t+T)$. Taking the Laplace transform on (3.40), we obtain

$$\widetilde{\mathbf{X}}(s) = (s^{\alpha}\mathbf{I} - \mathbf{A}(\mathbf{a}))^{-1}(s^{\alpha-1}\widetilde{\mathbf{x}}(T) + \mathcal{L}\left(\mathbf{h}(\widetilde{\mathbf{x}}(t+T);\mathbf{a})\right) + \mathcal{L}(\mathbf{g}(t+T;\mathbf{a}))\,) \tag{3.41}$$

where $\mathbf{I}$ is the 2×2 identity matrix. By using the inverse Laplace transform, the solution of (3.40) can be found

$$\begin{aligned} \widetilde{\mathbf{x}}(t+T) =& E_{\alpha,1}(t^{\alpha}\mathbf{A}(\mathbf{a}))\widetilde{\mathbf{x}}(T) \\ &+ \int_0^t (t-r)^{\alpha-1} E_{\alpha,\alpha}((t-r)^{\alpha}\mathbf{A}(\mathbf{a}))(\mathbf{h}(\widetilde{\mathbf{x}}(r+T);\mathbf{a}))dr \\ &+ \int_0^t (t-r)^{\alpha-1} E_{\alpha,\alpha}((t-r)^{\alpha}\mathbf{A}(\mathbf{a}))(\mathbf{g}(r+T;\mathbf{a}))dr. \end{aligned} \tag{3.42}$$

By using Lemma 3.3.12 and Lemma 3.3.14, there exist positive constants C and N such that

$$\begin{aligned} ||\widetilde{\mathbf{x}}(t+T)|| \;\leq\; & \frac{C||\widetilde{\mathbf{x}}(T)||}{1+||\mathbf{A}(\mathbf{a})||t^{\alpha}} + N \sup_{0\leq r\leq t} ||\mathbf{g}(r+T;\mathbf{a})|| \\ &+ \int_0^t ||(t-r)^{\alpha-1} E_{\alpha,\alpha}((t-r)^{\alpha}\mathbf{A}(\mathbf{a}))||\; ||\mathbf{h}(\widetilde{\mathbf{x}}(r+T);\mathbf{a})||dr. \end{aligned} \tag{3.43}$$

By the assumption and (3.39), we have

$$\frac{C||\widetilde{\mathbf{x}}(T)||}{1+||\mathbf{A}(\mathbf{a})||t^{\alpha}} + N \sup_{0\leq r\leq t} ||\mathbf{g}(r+T;\mathbf{a})|| < \epsilon\,(C||\widetilde{\mathbf{x}}(T)|| + Np_2^{\alpha}S_I)\,. \tag{3.44}$$

Since $||\mathbf{h}(\widetilde{\mathbf{x}}(t+T);\mathbf{a})||/||\widetilde{\mathbf{x}}(t+T)||$ tends to zero as $||\widetilde{\mathbf{x}}(t+T)||$ approaches zero, there exist constants $\delta, C_0 > 0$ such that

$$||\mathbf{h}(\widetilde{\mathbf{x}}(t+T);\mathbf{a})|| \leq C_0||\widetilde{\mathbf{x}}(t+T)|| \quad \text{as} \quad ||\widetilde{\mathbf{x}}(t+T)|| < \delta. \tag{3.45}$$

Substituting (3.45) into (3.43) and by (3.44), we get

$$\begin{aligned} ||\widetilde{\mathbf{x}}(t+T)|| \leq & \epsilon\left(C||\widetilde{\mathbf{x}}(T)|| + Np_2^{\alpha}S_I\right) \\ & + C_0\int_0^t ||(t-r)^{\alpha-1}E_{\alpha,\alpha}((t-r)^{\alpha}\mathbf{A}(\mathbf{a}))||\ ||\widetilde{\mathbf{x}}(r+T)||dr. \end{aligned} \tag{3.46}$$

Applying Lemma 3.3.15 to (3.46), we obtain

$$\begin{aligned} ||\widetilde{\mathbf{x}}(t+T)|| \leq & \epsilon\left(C||\widetilde{\mathbf{x}}(T)|| + Np_2^{\alpha}S_I\right) \\ & + C_0\int_0^t \epsilon\left(C||\widetilde{\mathbf{x}}(T)|| + Np_2^{\alpha}S_I\right)||(t-r)^{\alpha-1}E_{\alpha,\alpha}((t-r)^{\alpha}\mathbf{A}(\mathbf{a}))|| \\ & \times exp\Big\{C_0\int_r^t ||(t-s)^{\alpha-1}E_{\alpha,\alpha}((t-s)^{\alpha}\mathbf{A}(\mathbf{a}))||\Big\}dsdr. \end{aligned} \tag{3.47}$$

From Lemma 3.3.14, (3.47) gives

$$||\widetilde{\mathbf{x}}(t+T)|| \leq \epsilon\left(C||\widetilde{\mathbf{x}}(T)|| + Np_2^{\alpha}S_I\right) + C_0Ne^{C_0N}\epsilon\left(C||\widetilde{\mathbf{x}}(T)|| + Np_2^{\alpha}S_I\right). \tag{3.48}$$

Therefore, it immediately follows that $||\widetilde{\mathbf{x}}(t)||$ tends to zero as time goes to infinity. This proves the proposition. □

3.4 Numerical methods

The fractional Adams method is an effective technique for solving fractional-order differential equations [32, 33]. It is used for both linear and nonlinear problems, and can be extended to multi–term fractional–order differential

equations. In this section, we use this method to find the numerical solution of the nonlinear system (3.13). The idea of the method is to replace (3.13) by the equivalent fractional integral equations (3.30). We also use the method and algorithm in Section 2.1.4 to minimize the objective functional and to estimate the parameter values, respectively. The first four observed glucose data are excluded by setting their weights to zero.

The rest of this section is organized as follows. In Section 3.4.1, we introduce briefly the fractional Adams method [32, 33] and derive the predictor–corrector scheme for system (3.13). In order to use the nonlinear weighted least–squares method and the Levenberg–Marquardt algorithm, sensitivity equations are discussed in Section 3.4.2. In Section 3.4.3, the method for finding the optimal initial guess is presented.

3.4.1 The fractional Adams method

Consider the following fractional–order differential equation

$$ {}_C D_0^{\alpha} y(t) = f(t, y(t)), \quad y(0) = y_0. \tag{3.49} $$

Assume that the function f is continuous and satisfies a Lipschitz condition with respect to its second argument with Lipschitz constant L on a suitable set. Then there exists a unique solution y of the initial value problem (3.49) on some interval $[0, T]$ by the existence and uniqueness theorem for the Caputo's type of fractional–order differential equation [31]. The initial value problem (3.49) is equivalent to the Volterra integral equation

$$ y(t) = y_0 + \frac{1}{\Gamma(\alpha)} \int_0^t (t-u)^{\alpha-1} f(u, y(u)) du. \tag{3.50} $$

Set $h = \frac{T}{N},\ t_i = ih,\ i = 0, 1, \cdots, N$, where N is a positive integer. We apply the approximation

$$\int_0^{t_{k+1}} (t-u)^{\alpha-1} f(u, y(u))du \approx \int_0^{t_{k+1}} (t-u)^{\alpha-1} \tilde{f}_{k+1}(u, y(u))du, \tag{3.51}$$

where $\tilde{f}_{k+1}$ is the piecewise linear interpolant for f with node and knots chosen at the $t_i,\ i = 0, 1, 2, \cdots, k+1$. We can rewrite the integral on the right–hand side of (3.51) as

$$\int_0^{t_{k+1}} (t-u)^{\alpha-1} \tilde{f}_{k+1}(u, y(u))du = \sum_{i=0}^{k+1} a_{i,k+1} f(t_i, y(t_i)) \tag{3.52}$$

where

$$a_{i,k+1} = \frac{h^\alpha}{\alpha(\alpha+1)} \times \begin{cases} k^{\alpha+1} - (k-\alpha)(k+1)^\alpha, & i = 0, \\ (k-i+2)^{\alpha+1} + (k-i)^{\alpha+1} & \\ \qquad -2(k-i+1)^{\alpha+1}, & 1 \le i \le k, \\ 1, & i = k+1. \end{cases} \tag{3.53}$$

Then (3.50) can be discretized as follows:

$$y(t_{k+1}) \approx y_{k+1} = y_0 + \frac{1}{\Gamma(\alpha)} \Big(\sum_{i=0}^{k} a_{i,k+1} f(t_i, y(t_i)) + a_{k+1,k+1} f(t_{k+1}, y_{k+1}^P) \Big), \tag{3.54}$$

where y_{k+1} and y_{k+1}^P are the approximation and the predictor at time t_{k+1}, respectively. The remaining predictor y_{k+1}^P is calculated by the product rectangle rule,

$$\int_0^{t_{k+1}} (t-u)^{\alpha-1} f(u, y(u))du \approx \sum_{i=0}^{k} b_{i,k+1} f(t_i, y(t_i)), \tag{3.55}$$

where $b_{i,k+1} = \frac{h^\alpha}{\alpha}((k+1-i)^\alpha - (k-i)^\alpha)$. Therefore, the predictor y_{k+1}^P is obtained as follows:

$$y_{k+1}^P = y_0 + \frac{1}{\Gamma(\alpha)} \sum_{i=0}^{k} b_{i,k+1} f(t_i, y(t_i)). \tag{3.56}$$

The approximation method (3.54) leads to the following theorem for error bounds under smoothness assumptions on the solution.

Theorem 3.4.1. (Theorem 3.2. in [33]) *Let $\alpha > 0$ and assume that the function $f(t, y(t))$ in (3.49) is of class $C^2[0, T]$ for some suitable T. Then,*

$$\max_{0 \le i \le N} |y(t_i) - y_i| = \begin{cases} \mathcal{O}(h^2), & \text{if } \alpha \ge 1, \\ \mathcal{O}(h^{1+\alpha}), & \text{if } \alpha < 1. \end{cases} \tag{3.57}$$

Applying the method (3.54), (3.13) can be discretized as follows:

$$\begin{aligned} G_{k+1} &= G_0 + \frac{1}{\Gamma(\alpha)} \sum_{i=0}^{k} a_{1,i,k+1}[-({S_G}^\alpha + \tau^{1-\alpha} X_i) G_i + {S_G}^\alpha G_b] \\ &+ \frac{1}{\Gamma(\alpha)} a_{1,k+1,k+1}[-({S_G}^\alpha + \tau^{1-\alpha} X_{k+1}^P) G_{k+1}^P + {S_G}^\alpha G_b], \quad (3.58a) \\ X_{k+1} &= \frac{1}{\Gamma(\alpha)} \sum_{i=0}^{k} a_{2,i,k+1}[-{p_2}^\alpha (X_i - S_I (I_i - I_b)^+)] \\ &+ \frac{1}{\Gamma(\alpha)} a_{2,k+1,k+1}[-{p_2}^\alpha (X_{k+1}^P - S_I (I_{k+1} - I_b)^+)], \quad (3.58b) \end{aligned}$$

in which

$$G_{k+1}^{P} = G_0 + \frac{1}{\Gamma(\alpha)} \sum_{i=0}^{k} b_{1,i,k+1}[-({S_G}^{\alpha} + \tau^{1-\alpha} X_i) G_i + {S_G}^{\alpha} G_b],$$

$$X_{k+1}^{P} = \frac{1}{\Gamma(\alpha)} \sum_{i=0}^{k} b_{2,i,k+1}[-{p_2}^{\alpha}(X_i - S_I(I_i - I_b)^{+})],$$

$$a_{l,i,k+1} = \frac{h^{\alpha}}{\alpha(\alpha+1)} \times \begin{cases} k^{\alpha+1} - (k-\alpha)(k+1)^{\alpha}, & i = 0, \\ (k-i+2)^{\alpha+1} + (k-i)^{\alpha+1} & \\ \qquad -2(k-i+1)^{\alpha+1}, & 1 \le i \le k, \\ 1, & i = k+1, \end{cases}$$

$$b_{l,i,k+1} = \frac{h^{\alpha}}{\alpha}((k+1-i)^{\alpha} - (k-i)^{\alpha}),\ 0 \le i \le k,\ \text{and } l = 1, 2.$$

By using the derived discrete scheme (3.58), we find the numerical solution for the system (3.13).

3.4.2 Sensitivity equations

Recalling the natation (3.15), the nonlinear weighted least–squares method and the Levenberg–Marquardt algorithm require the partial derivatives of $\mathbf{x}(t)$ with respect to every single element of the parameter vector $\mathbf{a}$. In order to obtain the derivatives, we need to calculate the first derivatives of the model prediction $\mathbf{f}(t, \mathbf{x}; \mathbf{a})$ with respect to every single element of the parameter vector $\mathbf{a}$. And then interchanging the order of time and parameter derivatives, the fractional Adams method is applied. Therefore, we obtain the partial derivatives of $\mathbf{x}(t)$ with respect to every single element of the parameter vector $\mathbf{a}$. Our model (3.15) is not dynamically linear system, and therefore it is not possible to calculate the exact derivatives since the dependency of $\mathbf{f}(t, \mathbf{x}; \mathbf{a})$ on parameters $\mathbf{a}$ is unknown. In particular, derivatives of (3.13a) and (3.13b)

are taken with respect to S_G, p_2, S_I, G_0, τ, α, and the following system is obtained:

$$
\begin{aligned}
\frac{\partial {}_C D_0^\alpha G(t)}{\partial S_G} &= -({S_G}^\alpha + \tau^{1-\alpha} X(t)) \frac{\partial G(t)}{\partial S_G} + \alpha {S_G}^{\alpha-1}(G_b - G(t)), && \frac{\partial G(t)}{\partial S_G}\Big|_{t=0} = 0,\\
\frac{\partial {}_C D_0^\alpha G(t)}{\partial p_2} &= -({S_G}^\alpha + \tau^{1-\alpha} X(t)) \frac{\partial G(t)}{\partial p_2} - \tau^{1-\alpha} G(t) \frac{\partial X(t)}{\partial p_2}, && \frac{\partial G(t)}{\partial p_2}\Big|_{t=0} = 0,\\
\frac{\partial {}_C D_0^\alpha G(t)}{\partial S_I} &= -({S_G}^\alpha + \tau^{1-\alpha} X(t)) \frac{\partial G(t)}{\partial S_I} - \tau^{1-\alpha} G(t) \frac{\partial X(t)}{\partial S_I}, && \frac{\partial G(t)}{\partial S_I}\Big|_{t=0} = 0,\\
\frac{\partial {}_C D_0^\alpha G(t)}{\partial G_0} &= -({S_G}^\alpha + \tau^{1-\alpha} X(t)) \frac{\partial G(t)}{\partial G_0}, && \frac{\partial G(t)}{\partial G_0}\Big|_{t=0} = 1,\\
\frac{\partial {}_C D_0^\alpha G(t)}{\partial \tau} &= -({S_G}^\alpha + \tau^{1-\alpha} X(t)) \frac{\partial G(t)}{\partial \tau} - (1-\alpha)\tau^{-\alpha} X(t) G(t), && \frac{\partial G(t)}{\partial \tau}\Big|_{t=0} = 0,\\
\frac{\partial {}_C D_0^\alpha G(t)}{\partial \alpha} &= -({S_G}^\alpha + \tau^{1-\alpha} X(t)) \frac{\partial G(t)}{\partial \alpha} - \tau^{1-\alpha} G(t) \frac{\partial X(t)}{\partial \alpha} \\
&\quad - ({S_G}^\alpha \log S_G - \tau^{1-\alpha} X(t) \log \tau) G(t) + {S_G}^\alpha G_b \log S_G, && \frac{\partial G(t)}{\partial \alpha}\Big|_{t=0} = 0,\\
\frac{\partial {}_C D_0^\alpha X(t)}{\partial S_G} &= 0, \\
\frac{\partial {}_C D_0^\alpha X(t)}{\partial p_2} &= -{p_2}^\alpha \frac{\partial X(t)}{\partial p_2} - \alpha {p_2}^{\alpha-1}(X(t) - S_I(I(t) - I_b)^+), && \frac{\partial X(t)}{\partial p_2}\Big|_{t=0} = 0,\\
\frac{\partial {}_C D_0^\alpha X(t)}{\partial S_I} &= -{p_2}^\alpha \frac{\partial X(t)}{\partial S_I} + {p_2}^\alpha (I(t) - I_b)^+, && \frac{\partial X(t)}{\partial S_I}\Big|_{t=0} = 0,\\
\frac{\partial {}_C D_0^\alpha X(t)}{\partial G_0} &= 0, \\
\frac{\partial {}_C D_0^\alpha X(t)}{\partial \tau} &= 0, \\
\frac{\partial {}_C D_0^\alpha X(t)}{\partial \alpha} &= -{p_2}^\alpha \frac{\partial X(t)}{\partial \alpha} - {p_2}^\alpha \log p_2 (X(t) - S_I(I(t) - I_b)^+), && \frac{\partial X(t)}{\partial \alpha}\Big|_{t=0} = 0.
\end{aligned}
\tag{3.59}
$$

3.4.3 Initial estimates for parameters and the optimal fractional order

It is important but difficult to determine an initial guess for each parameter in the nonlinear model. We consider a number of initialization approaches for obtaining optimal model parameters.

In non–diabetics, we divide the ranges of S_G, S_I, p_2, and G_0 in Table 2.13 into nineteen equal parts. The range of τ, for considering the increase and de-

crease of the exponential function, is set to $(0.1, 2)$ and separated into nineteen equal parts. Also, to find the optimal fractional order, the same process is performed in the range $(0.1, 1)$ of the fractional order α. From those, we consider the number of twenty initial estimates for each parameter. For example, for parameter G_0, we think the initial estimates $150 + \frac{k}{19}(400 - 150)$, $k = 1, \cdots, 19$. In the original case ($\alpha = 1$), the initial estimate for τ is meaningless. Therefore, we estimate the parameters $20^5 \cdot 19 + 20^4$ times. From these, we choose the parameters generating the smallest chi–square value, which is given by $\chi^2 = \sum_{i=1}^{n}(y_i - \bar{y}(t_i; \vec{a}))^2/{\sigma_i}^2$, where n is the number of data, y_i and $\bar{y}$ are the observed datum and the numerical solution at time t_i, respectively, $\vec{a} = (a_i)_{i=1}^{m}$ is the set of parameters, and σ_i is the standard deviation associated with each measurement y_i. The relative l_2 error is calculated by $\frac{\sqrt{\chi^2}}{\sqrt{\sum_{i=1}^{n} {y_i}^2}}$. In order to shorten computation times, we have used MPI (Message Passing Interface) [75]

In diabetes patients, we determine and use parameter ranges that cover the extreme cases referenced in [99]. The ranges of parameters S_G and p_2 are identical to those in the non–diabetic case. However, the ranges of S_I and G_0 are changed to (0.05e−04, 7.00e−04) and (200, 450), respectively. The rest of this process is the same as for non–diabetics.

3.5 Numerical results

In this section, we present some numerical results obtained from the fractional-order MINMOD Millennium. We apply eight subjects to this model, including type 2 diabetic patients as well as non–diabetic subjects. In Table 3.1, each column gives the source, type, experimental test, and clinical basal values for each subject. In the third column, Normal and Patient represent subject for non–diabetic and patient with type 2 diabetes, respectively. FSIGT and

IM–FSIGT are explained in Section 1.1 and Section 2.1. The FSIGT with tolbutamide involves an additional injection of tolbutamide over 20 s, 20 min after the glucose injection. For detailed information for the types and tests, see the references in the source.

Subject	Source	Type	Test	Clinical basal values	
				G_b	I_b
1	[76]	Normal	FSIGT	92.00	7.30
2	[66]	Normal	IM–FSIGT	89.75	11.00
3	[84]	Normal	IM–FSIGT	78.00	9.00
4	[77]	Normal	FSIGT	87.00	6.00
5	[77]	Normal	IM–FSIGT	89.00	7.00
6	[8]	Normal	FSIGT with tolbutamide	97.00	17.00
7	[99]	Normal	IM–FSIGT	82.00	11.00
8	[99]	Patient	IM–FSIGT	193.00	56.00

Table 3.1: Type and test for each subject.

Figure 3.2 shows the experimental values of glucose and insulin with simulated glucose concentration. Also, the estimated optimal fractional order α for each subject is shown. As we can see, the numerical results fit the experimental data well, including diabetic patients. For those data produced by IM–FSIGT, we observe the small peaks near 20 min due to the administration of insulin (See Figure 3.2b, Figure 3.2c, Figure 3.2e, Figure 3.2f, Figure 3.2g, and Figure 3.2h.). From Figure 3.2g and Figure 3.2h, we see that patients with diabetes have higher basal, peak glucose values and higher basal insulin compared to normal subjects. And we can observe that the glucose concentrations have positive values and converge to their basal line (G_b) in all numerical results. Hence, we have verified the mathematical analysis presented in Proposition 3.3.13 and Proposition 3.3.16. In Table 3.3, the optimal fractional order, the estimated parameters, and the relative l_2 error for each subject are given. Compared to the values in Table 3.2, they not only produce

almost the smallest chi–square value, but also represent the rheological behavior of glucose–insulin. Among them, we are most interested in the estimating the value of parameter S_I, because it is the most important factor determining glucose tolerance [7]. It is well known that diabetic patients have significantly more insulin resistant (lower S_I) than the normal subjects [11, 40, 45, 50, 99]. From Table 3.3, we have confirmed the same phenomena regardless of design and method in our research. Comparing subject 7 to 8, we can conclude that S_G in diabetics is also significantly lower than S_G in non–diabetics. In addition, the S_G in subject 4 shows the possibility of the insufficient glucose disappearance.

In Table 3.3, we also find that the value of $\tau^{1-\alpha}$ in diabetics is significantly higher than that in non–diabetics. To understand the relationship between $\tau^{1-\alpha}$ and S_I, we estimated the parameters with fixed $\tau^{1-\alpha} = 1.00$ (normal subjects) and $\tau^{1-\alpha} = 2.00$ (diabetic patients). Parameters α, S_G, p_2, and G_0 are similar. However, the value of S_I is increasing (decreasing) when the value of $\tau^{1-\alpha}$ is decreasing (increasing) (See Table 3.3 and Table 3.4). It should be noted that the values of product $S_I \cdot \tau^{1-\alpha}$ are almost constant in all tables. In (3.13), the strong effect of S_I is derived from the large difference of $(I(t) - I_b)$ in the early time, and it has a big impact on the value of $X(t)$. Simultaneously, from Remark 3.3.3, we can physiologically consider $\tau^{1-\alpha}$ as the effect of the rheological behavior in increasing the muscular and liver sensibility to the action of insulin [6, 7, 28]. This means that the more the decrease of insulin sensitivity (S_I), the more the need of the active rate ($\tau^{1-\alpha}$) to maintain the balance of glucose–insulin. For those reasons, the value of S_I is inversely proportional to the value of $\tau^{1-\alpha}$. Therefore, we can conclude that the value of $\tau^{1-\alpha}$ in diabetics is higher than that in non–diabetics and $S_I \cdot \tau^{1-\alpha}$ remains to be almost constant.

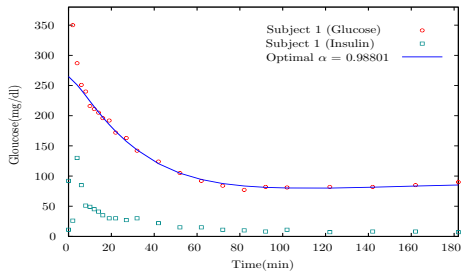

(a) Subject 1.

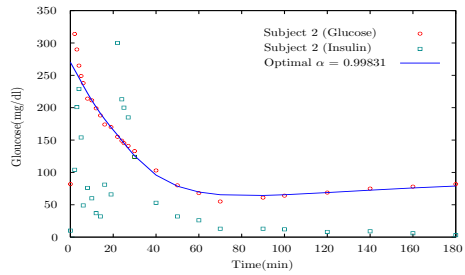

(b) Subject 2.

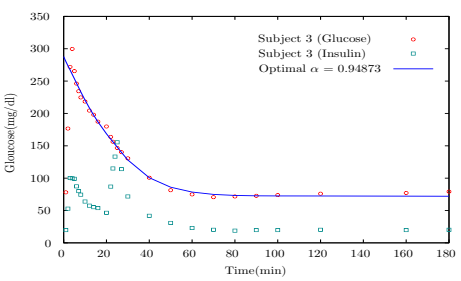

(c) Subject 3.

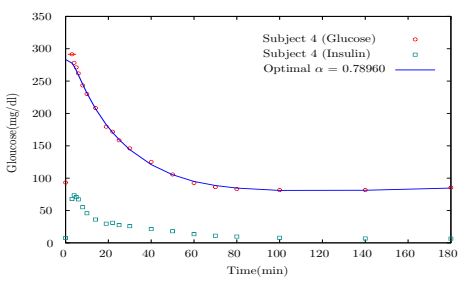

(d) Subject 4.

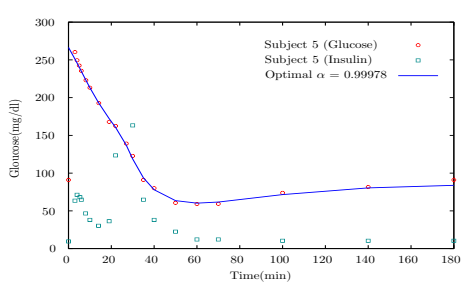

(e) Subject 5.

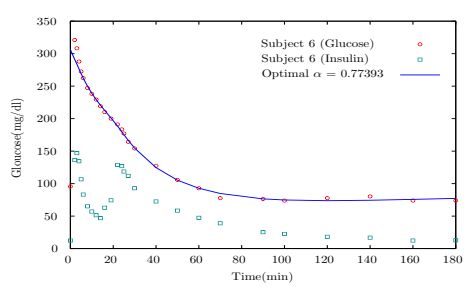

(f) Subject 6.

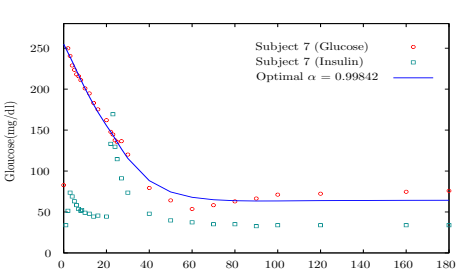

(g) Subject 7.

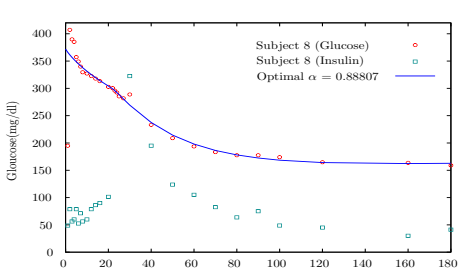

(h) Subject 8.

Figure 3.2: Plots with experimental and computed values for subjects.

Subject	Order α	Estimated parameters				Relative l_2 error
		S_G	p_2	S_I	G_0	
1	1.00	0.20437e−01	0.29249e−01	0.57313e−03	264.92	2.66e−02
2	1.00	0.33801e−01	0.16086e−01	0.44230e−03	270.07	3.21e−02
3	1.00	0.33628e−01	0.56249e−01	0.22334e−03	287.20	3.02e−02
4	1.00	0.38406e−01	0.16033e−01	0.40537e−03	304.09	1.47e−02
5	1.00	0.29322e−01	0.59264e−01	0.37933e−03	266.55	2.01e−02
6	1.00	0.30859e−01	0.10191e−01	0.50573e−03	298.85	1.95e−02
7	1.00	0.31191e−01	0.66875e−01	0.36755e−03	255.56	4.50e−02
8	1.00	0.23430e−01	0.76598e−02	0.11648e−03	368.64	2.17e−02

Table 3.2: Estimated parameters, and relative l_2 error for each subject when $\alpha = 1.00$.

3.6 Conclusions

In this paper, to represent the rheological behavior of glucose–insulin, we have introduced a fractional order ($0 < \alpha \leq 1$) into MINMOD Millennium. In Section 3.3, we showed that our model (3.13) has non–negative, bounded solutions and a locally asymptotically stable equilibrium points. Applying the initial guesses for each parameter in Section 3.4, we obtained the optimal fractional order and estimated parameters for each set of subjects, including type 2 diabetic patients. From the numerical results in Section 3.5, we can confirm that insulin sensitivity (S_I) is significantly lower in diabetics than in non–diabetics. In addition, we found the relation between S_I and $\tau^{1-\alpha}$, thus, we conclude $\tau^{1-\alpha}$ is the affecting factor for determining glucose tolerance. Further research is required to study the application to other many subjects (including type 1 diabetic patients) and establish ranges of parameters for the model.

Subject	Estimated parameters						$S_I \cdot \tau^{1-\alpha}$	Relative l_2 error
	Optimal order α	S_G	p_2	S_I	G_0	$\tau^{1-\alpha}$		
1	0.98801	0.19086e−01	0.28941e−01	0.54737e−03	264.88	1.18	6.44e−04	2.69e−02
2	0.99831	0.33715e−01	0.16041e−01	0.43930e−03	270.15	1.02	4.47e−04	3.21e−02
3	0.94873	0.29310e−01	0.49652e−01	0.33898e−03	287.81	1.15	3.90e−04	3.00e−02
4	0.78960	0.77217e−03	0.20378e−01	0.28824e−02	283.45	1.30	3.69e−03	1.24e−02
5	0.99978	0.29255e−01	0.59440e−01	0.37828e−03	266.46	1.00	3.79e−04	2.01e−02
6	0.77393	0.14126e−01	0.55381e−02	0.21165e−02	305.96	1.39	2.93e−03	1.64e−02
7	0.99842	0.30428e−01	0.71303e−01	0.36552e−03	254.98	1.01	3.68e−04	4.50e−02
8	0.88807	0.20880e−01	0.33804e−02	0.20617e−03	372.05	1.87	3.85e−04	2.02e−02

Table 3.3: Optimal order ($0 < \alpha < 1$), estimated parameters, and relative l_2 error for each subject.

Remark 3.5.1. *In Table 3.3, we consider the value of* $\tau^{1-\alpha}$ *because* τ *may not have any meaning when the value of* α *reaches* 1.00.

Subject	Estimated parameters							Relative
	Optimal order α	S_G	p_2	S_I	G_0	$\tau^{1-\alpha}$	$S_I \cdot \tau^{1-\alpha}$	l_2 error
1	0.99288	0.19661e−01	0.29029e−01	0.61453e−03	264.92	1.00	6.15e−04	2.68e−02
2	0.99998	0.33800e−01	0.16086e−01	0.44235e−03	270.07	1.00	4.42e−04	3.21e−02
3	0.94873	0.29310e−01	0.49652e−01	0.39021e−03	287.81	1.00	3.90e−04	3.00e−02
4	0.78599	0.88965e−03	0.19449e−01	0.38177e−02	284.19	1.00	3.82e−03	1.24e−02
5	0.99998	0.29317e−01	0.59272e−01	0.37938e−03	266.54	1.00	3.79e−04	2.01e−02
6	0.77394	0.14127e−01	0.55385e−02	0.29340e−02	305.96	1.00	2.93e−03	1.64e−02
7	0.99984	0.31021e−01	0.68040e−01	0.36742e−03	255.46	1.00	3.67e−04	4.50e−02
8	0.88808	0.20880e−01	0.33805e−02	0.19246e−03	372.05	2.00	3.84e−04	2.02e−02

Table 3.4: Optimal order ($0 < \alpha < 1$), estimated parameters, and relative l_2 error for each subject when $\tau^{1-\alpha} = 1.00$ (normal subjects) or 2.00 (diabetic patients)

.

Bibliography

[1] N. H. Abel. *Solution de quelques problèmes à l'aide d'intégrales définies, Oeuvres Complètes*, volume 1. Grøndahl, Christiania, Norway, 1881.

[2] T. J. Anastasio. The fractional-order dynamics of brainstem vestibulo-oculomotor neurons. *Biol. Cybern.*, 72:69–79, 1994.

[3] China faces 'diabetes epidemic', research suggests. BBC. March 25, 2010. Online; accessed 20-May-2013.

[4] R. N. Bergman. Lilly lecture 1989. Toward physiological understanding of glucose tolerance. Minimal-model approach. *Diabetes*, 38:1512–1527, 1989.

[5] R. N. Bergman. The minimal model: Perspective from 2005. *Horm. Res.*, 64:8–15, 2005.

[6] R. N. Bergman, Y. Z. Ider, C. R. Bowden, and C. Cobelli. Quantitative estimation of insulin sensitivity. *Am. J. Physiol-Endoc. M.*, 236:E667–E677, 1979.

[7] R. N. Bergman, L. S. Phillips, and C. Cobelli. Physiologic evaluation of factors controlling glucose tolerance in man: measurement of insulin

sensitivity and β-cell glucose sensitivity from the response to intravenous glucose. *J. Clin. Invest.*, December 68(6):1456–1467, 1981.

[8] R. N. Bergman, R. Prager, A. Volund, and J. M. Olefsky. Equivalence of the insulin sensitivity index in man derived by the minimal model method and the euglycemic glucose clamp. *J. Clin. Invest.*, 79(3):790–800, 3 1987.

[9] G. W. S. Blair. The role of psychophysics in rheology. *J. Coll. Sci. Imp. U. Tok.*, pages 21–32, 1947.

[10] India's Diabetes Epidemic Cuts Down Millions Who Escape Poverty. Bloomberg Markets Magazine. November 08, 2010. Online; accessed 20-May-2013.

[11] E. Bonora, G. Targher, M. Alberiche, R. C. Bonadonna, F. Saggiani, M. B. Zenere, T. Monauni, and M. Muggeo. Homeostasis model assessment closely mirrors the glucose clamp technique in the assessment of insulin sensitivity: studies in subjects with various degrees of glucose tolerance and insulin sensitivity. *Diabetes Care*, 23(1):57–63, 2000.

[12] R. C. Boston and P. J. Moate. A novel minimal model to describe nefa kinetics following an intravenous glucose challenge. *Am. J. Physiol-Reg. I.*, 294:R1140–R1147, 2008.

[13] R. C. Boston, D. Stefanovski, P. J. Moate, A. E. Sumner, R. M. Watanabe, and R. N. Bergman. MINMOD Millennium: A computer program to calculate glucose effectiveness and insulin sensitivity from the frequently sampled intravenous glucose tolerance test. *Diabetes. Technol. The.*, 5:1003–1015, 2003.

[14] A. Boutayeb and A. Chetouani. A critical review of mathematical models and data used in diabetology. *Biomed. Eng. Online.*, 5:43, 2006.

[15] R. Bruce, I. Godsland, C. Walton, D. Crook, and V. Wynn. Associations between insulin sensitivity, and free fatty acid and triglyceride metabolism independent of uncomplicated obesity. *Metabolis.*, l43(10):1275–1281, 1994.

[16] R. Burden, J. Faires, and A. Reynolds. *Numerical Analysis, 2nd Edn.* Prindle Weber and Schmidt, Boston MA, 1980.

[17] M. Caputo and F. Mainardi. A new dissipation model based on memory mechanism. *Pure. Appl. Geophys.*, 91:134–147, 1971.

[18] Number of Americans with Diabetes Rises to Nearly 26 Million. Centers for Disease Control and Prevention, Online; accessed 20-May-2013.

[19] Y. Cho. A Comparison of Several Mathematical Glucose–insulin. Unpublished master's thesis, Seoul National University, 2010.

[20] Y. Cho, I. Kim, and D. Sheen. A fractional–order model for MINMOD Millennium. Preprint.

[21] Y. Cho, I. Kim, and D. Sheen. Glucose–insulin dynamics and its parameter estimation. Submitted.

[22] K. S. Cole. Electric conductance of biological systems. *Cold spring. Harb. Sym.*, 1:107–116, 1933.

[23] P. J. Coon, E. M. Rogus, and A. P. Goldberg. Time course of plasma free fatty acid concentration in response to insulin: Effect of obesity and physical fitness. *Metabolis.*, 41(7):711–716, 1992.

[24] L. Coppola, G. Verrazzo, C. La Marca, P. Ziccardi, A. Grassia, A. Tirelli, and D. Giugliano. Effect of insulin on blood rheology in non-diabetic subjects and in patients with type 2 diabetes mellitus. *Diabetic Med.*, 14(11):959–963, 1997.

[25] A. De Gaetano and O. Arino. Mathematical modeling of the intravenous glucose tolerance test. *J. Math. Biol.*, 40:136–168, 2000.

[26] A. De Morgan. *The Differential and Integral Calculus Combining Differentiation, Integration, Development, Differential Equations, Differences, Summation, Calculus of Variations ...with Applications to Alebra, Plane and Solid Geometry.* Baldwin and Craddock, London; published in 25 parts under the superintendence of the Society for the Diffusion of Useful Knowledge, 1840.

[27] P. Dejkhamron, R. K. Menon, and M. A. Sperling. Childhood diabetes mellitus: Recent advances and future prospects. *Indian J. Med. Res.*, 125(3):231–250, 2007.

[28] M. Derouich and A. Boutayeb. The effect of physical exercise on the dynamics of glucose and insulin. *J. Biomech.*, 35:911–917, 2002.

[29] Diabetes in India. Diabetes. co. uk the global diabetes community, Online; accessed 20-May-2013.

[30] Diagnosis and Classification of Diabetes Mellitus, 2004.

[31] K. Diethelm. *The Analysis of Fractional Differential Equations : An Application-Oriented Exposition Using Differential Operators of Caputo Type.* Lecture Notes in Mathematics;2004. Springer-Verlag Berlin Heidelberg, Berlin, Heidelberg, 2010.

[32] K. Diethelm, N. Ford, and A. Freed. A predictor-corrector approach for the numerical solution of fractional differential equations. *Nonliear Dynam.*, 29:3–22, 2002.

[33] K. Diethelm, N. J. Ford, and A. D. Freed. Detailed error analysis for a fractional adams method. *Numer. Algorithms.*, 36:31–52, 2004.

[34] Y. Ding and H. Ye. A fractional-order differential equation model of HIV infection of $CD4^+$ t-cells. *Math. Comput. Model.*, 50(3–4):386–392, 2009.

[35] V. D. Djordjević, J. Jarić, B. Fabry, J. Fredberg, and D. Stamenović. Fractional derivatives embody essential features of cell rheological behavior. *Ann. Biomed. Eng.*, 31:692–699, 2003.

[36] D. M. Eddy and L. Schlessinger. Archimedes. *Diabetes Care*, 26(11):3093–3101, 2003.

[37] N. Engheta. On fractional calculus and fractional multipoles in electromagnetism. *IEEE T. Antenn. Propag.*, 44(4):554–566, APR 1996.

[38] A. Erdélyi, W. Magnus, F. Oberhettinger, and F. G. Tricomi. *Higher Transcendental Functions*, volume 3. McGraw–Hill, New York, 1955.

[39] L. Euler. De progressionibus transcendentibus, sev quarum terminigenerales algebraice dari nequent. *Commentarii Academiae Scientiarum Imperialis Scientiarum Petropolitanae*, 5:55, 1738.

[40] D. T. Finegood, I. M. Hramiak, and J. Dupre. A modified protocol for estimation of insulin sensitivity with the minimal model of glucose kinetics in patients with insulin-dependent diabetes. *J. Clin. Endocr. Metab.*, 70(6):1538–1549, 1990.

[41] R. A. Fletcher. *A modified Marquardt subroutine for nonlinear least squares*. United Kingdom Atomic Energy Authority, 1971.

[42] J. B. J. Fourier. *Théorie analytique de la chaleur, Oeuvres de Fourier*, volume 1. Firmin Didot, Paris, 1822.

[43] A. D. Gaetano and O. Arino. A statistical approach to the determination of stability for dynamical systems modelling physiological processes. *Math. Comput. Model.*, 31(4–5):41–51, 2000.

[44] A. N. Gerasimov. A generalization of linear laws of deformation and its application to problems of internal friction. *Akad. Nauk SSSR. Prikl.Mat.Meh.*, pages 251–260 (Russian), 1948.

[45] B. J. Goldstein. Insulin resistance as the core defect in type 2 diabetes mellitus. *Am. J. Cardiol.*, 90(5, Supplement 1):3–10, 2002.

[46] R. Gorenflo and F. Mainardi. *Fractional Calculus: Integral and Differential Equations of Fractional Order*. Fractals and Fractional Calculus in Continuum Mechanics. Springer, Wien, 1997.

[47] A. V. Hill. The possible effects of the aggregation of the molecules of haemoglobin on its dissociation curves. *J. Physiol.*, 40(Suppl):iv–vii, 1910.

[48] B. V. Howard, I. Klimes, B. Vasquez, D. Brady, M. Nagulesparan, and R. H. Unger. The antilipolytic action of insulin in obese subjects with resistance to its glucoregulatory action. *J. Clin. Endocr. Metab.*, 58(3):544–548, 1984.

[49] G. S. Jones. Fundamental Inequalities for Discrete and Discontinuous Functional Equations. *J. Soc. Ind. Appl. Math.*, 12(1):43–57, 1964.

[50] A. Katz, S. S. Nambi, K. Mather, A. D. Baron, D. A. Follmann, G. Sullivan, and M. J. Quon. Quantitative insulin sensitivity check index: A simple, accurate method for assessing insulin sensitivity in humans. *J. Clin. Endocr. Metab.*, 85(7):2402–2410, 2000.

[51] H. Khalil. *Nonlinear Systems*. Prentice Hall, 1996.

[52] S. F. Lacroix. *Traité du calcul différentiel et du calcul integral*. Courcier, Paris, 2 edition, 1819.

[53] D. E. Larson-Meyer, L. K. Heilbronn, L. M. Redman, B. R. Newcomer, M. I. Frisard, S. Anton, S. R. Smith, A. Alfonso, and E. Ravussin. Effect of calorie restriction with or without exercise on insulin sensitivity, β-cell function, fat cell size, and ectopic lipid in overweight subjects. *Diabetes Care*, 29(6):1337–1344, June 2006.

[54] M. Laville, V. Rigalleau, J. P. Riou, and M. Beylot. Respective role of plasma nonesterified fatty acid oxidation and total lipid oxidation in lipid-induced insulin resistance. *Metabolis.*, 44(5):639–644, 1995.

[55] G. W. Leibniz. Letter from Hanover, Germany, to G. F. A. L'Hôpital, September 30, 1695. *Mathematische Schriften*, 1849. reprinted 1962, Olms Verlag, Hildesheim, Germany, 2, 301–302.

[56] G. W. Leibniz. Letter from Hanover, Germany, to Johann Bernoulli, December 28, 1695. *Mathematische Schriften*, 1849. reprinted 1962, Olms Verlag, Hildesheim, Germany, 3, 226.

[57] G. W. Leibniz. Letter from Hanover, Germany, to John Wallis, May 28, 1697. *Mathematische Schriften*, 1849. reprinted 1962, Olms Verlag, Hildesheim, Germany, 4, 25.

[58] Y. Li, Y. Chen, and I. Podlubny. Mittag–Leffler stability of fractional order nonlinear dynamic systems. *Automatica*, 45(8):1965 – 1969, 2009.

[59] B. Liemann. *Versuch einer allgemeinen Auffassung der Integration und Differentiation, Gesammelte Werke.* published posthumously, Teubner, Leipzig, 1892.

[60] W. Lin. Global existence theory and chaos control of fractional differential equations. *J. Math. Anal. Appl.*, 332(1):709–726, 2007.

[61] S. MacRury and G. Lowe. Blood rheology in diabetes mellitus. *Diabetic Med.*, 7(4):285–291, 1990.

[62] A. Makroglou, J. Li, and Y. Kuang. Mathematical models and software tools for the glucose-insulin regulatory system and diabetes: an overview. *Appl. Numer. Math.*, 56:559–573, 2006.

[63] D. W. Marquardt. An algorithm for least-squares estimation of nonlinear parameters. *J. Soc. Ind. Appl. Math.*, 11(2):431–441, 1963.

[64] A. L. Mehaute and G. Crepy. Introduction to transfer and motion in fractal media: The geometry of kinetics. *Solid State Ionics*, 9–10, Part 1:17–30, 1983.

[65] K. S. Miller and B. Ross. *An Introduction to the Fractional Calculus and Fractional Differential Equations.* John Wiley & Sons, 1 edition, 1993.

[66] A Demo version 5.10 of MINMOD Millennium program, http://research.vet.upenn.edu/ biomath/ CurrentProjects/DiabetesGlucoseMetabolism/tabid/1622/Default.aspx. Accessed: 27/02/2013.

[67] A. Moan, G. Nordby, I. Os, K. I. Birkeland, and S. E. Kjeldsen. Relationship between hemorrheologic factors and insulin sensitivity in healthy young men. *Metabolis.*, 43(4):423–427, 1994.

[68] P. J. Moate, J. R. Roche, L. M. Chagas, and R. C. Boston. Evaluation of a compartmental model to describe non-esterified fatty acid kinetics in Holstein dairy cows. *J. Dairy. Res.*, 74(4):430–437, 2007.

[69] A. Mukhopadhyay, A. D. Gaetano, and O. Arino. *Modelling the intraveneous glucose tolerence test:A global study for single-distributed-delay model.* Discrete & Continuous Dynamical Sytems Series B 4(2) 407-417, 2004.

[70] R. R. Nigmatullin and S. O. Nelson. Recognition of the "fractional" kinetics in complex systems: dielectric properties of fresh fruits and vegetables from 0.01 to $1.8ghz$. *Signal Process.*, 86(10):2744–2759, October 2006.

[71] J. Norman. Normal regulation of blood glucose. http://www.endocrineweb.com/conditions/diabetes/normal-regulation-blood-glucose, 2011.

[72] Z. M. Odibat and N. T. Shawagfeh. Generalized taylor's formula. *Appl. Math. Comput.*, 186(1):286 – 293, 2007.

[73] K. B. Oldham and J. Spanier. The replacement of fick's laws by a formulation involving semidifferentiation. *J. Electroanal. Chem. and Interfacial Electrochem.*, 26(2–3):331–341, 1970.

[74] A. Oustaloup. *La dérivation non entière: théorie, synthèse et applications.* Hermes Science Publications, 1995.

[75] P. S. Pacheco. *Parallel programming with MPI.* Morgan Kaufmann Publishers Inc., San Francisco, CA, USA, 1996.

[76] G. Pacini and R. N. Bergman. MINMOD: A computer program to calculate insulin sensitivity and pancreatic responsivity from the frequently sampled intravenous glucose tolerance test,. *Comput. Meth. Prog. Bio.*, 23(2):113–122, 1986.

[77] G. Pacini, G. Tonolo, M. Sambataro, M. Maioli, M. Ciccarese, E. Brocco, A. Avogaro, and R. Nosadini. Insulin sensitivity and glucose effectiveness: minimal model analysis of regular and insulin-modified fsigt. *Am. J. Physiol-endoc. M.*, 274(4):E592–E599, 1998.

[78] A. Perez-Martin, M. Dumortier, E. Pierrisnard, E. Raynaud, J. Mercier, and J. Brun. Multivariate analysis of relationships between insulin sensitivity and blood rheology: Is plasma viscosity a marker of insulin resistance? *Clin. Hemorheol.*, 25(3–4):91–103, 2001.

[79] V. Periwal, C. C. Chow, R. N. Bergman, M. Ricks, G. L. Vega, and A. E. Sumner. Evaluation of quantitative models of the effect of insulin on lipolysis and glucose disposal. *Am. J. Physiol-Reg. I.*, 295(4):R1089–R1096, 2008.

[80] I. Podlubny. *Fractional Differential Equations.* Academic Press, San Diego, CA, USA, 1999.

[81] I. Podlubny. Fractional-order systems and $PI^{\lambda}D^{\mu}$-controllers. *IEEE T. Automat. Contr.*, 44(1):208–214, JAN 1999.

[82] N. M. Punjabi and B. A. Beamer. Alterations in glucose disposal in sleep-disordered breathing. *Am. J. Resp. Crit. Care.*, 179(3):235–240, 2009.

[83] D. Qian, C. Li, R. P. Agarwal, and P. J. Wong. Stability analysis of fractional differential system with Riemann–Liouville derivative. *Math. Comput. Model.*, 52(5–6):862– 874, 2010.

[84] M. Quon, C. Cochran, S. Taylor, and R. Eastman. Direct comparison of standard and insulin modified protocols for minimal model estimation of insulin sensitivity in normal subjects. *Diabetes Res.*, 25:139–149, 1994.

[85] A. Roy and R. S. Parker. Dynamic modeling of free fatty acid, glucose, and insulin: An extended minimal model. *Diabetes. Technol. The.*, 8(6):617–626, 2006.

[86] A. Roy and R. S. Parker. Dynamic modeling of exercise effects on plasma glucose and insulin levels. *J. Diabetes Sci. Technol.*, 1(3):338–347, 2007.

[87] R. D. Rudic, P. McNamara, A.-M. Curtis, R. C. Boston, S. Panda, J. B. Hogenesch, and G. A. FitzGerald. Bmal1 and clock, two essential components of the circadian clock, are involved in glucose homeostasis. *Plos. Biol.*, 2:e337, 2004.

[88] M. F. Saad, G. M. Steil, M. Riad-Gabriel, A. Khan, A. Sharma, R. Boyadjian, S. D. Jinagouda, and R. N. Bergman. Method of insulin administration has no effect on insulin sensitivity estimates from the insulin-modified minimal. *Diabetes*, pages 2044–2048, 1997.

[89] J. A. Seibel. Risk factors for diabetes. http://diabetes.webmd.com/risk-factors-for-diabetes, February 25, 2010.

[90] E. D. Smith, F. Szidarovszky, W. J. Karnavas, and A. T. Bahill. Sensitivity analysis, a powerful system validation technique. *The Open Cybernetics and Systemics Journal*, 2:39–56, 2008.

[91] N. Y. Sonin. *On differentiation with arbitrary index*, volume 6. Moscow Mat. Sb., 1869.

[92] R. Srinivasan, A. H. Kadish, and R. Sridhar. A mathematical model for the control mechanism of free fatty acid-glucose metabolism in normal humans. *Comput. Biomed. Res.*, 3(2):146–165, 1970.

[93] S. Srinivasan, G. R. Ambler, L. A. Baur, S. P. Garnett, M. Tepsa, F. Yap, G. M. Ward, and C. T. Cowell. Randomized, controlled trial of metformin for obesity and insulin resistance in children and adolescents: Improvement in body composition and fasting insulin. *J. Clin. Endocr. Metab.*, 91(6):2074–2080, 2006.

[94] H. O. Steinberg, G. Paradisi, G. Hook, K. Crowder, J. Cronin, and A. D. Baron. Free fatty acid elevation impairs insulin-mediated vasodilation and nitric oxide production. *Diabetes*, 49(7):1231–1238, 2000.

[95] T. Szkudelski and K. Szkudelska. Glucose as a lipolytic agent: Studies on isolated rat adipocytes. *Physiol. Res.*, 49:213–217, 2000.

[96] D. Thiébaud, R. A. DeFronzo, E. Jacot, A. Golay, K. Acheson, E. Maeder, E. Jéquier, and J. P. Felber. Effect of long chain triglyceride infusion on glucose metabolism in man. *Metabolis.*, 31(11):1128–1136, 1982.

[97] K. Thomaseth and A. Pavan. Model-based analysis of glucose and free fatty acid kinetics during glucose tolerance tests. In *Mathematical Modeling in Nutrition and Toxicology*, pages 21–40, Athens, GA, USA, 2005.

[98] G. Toffolo, R. N. Bergman, D. T. Finegood, C. R. Bowden, and C. Cobelli. Quantitative estimation of beta cell sensitivity to glucose in the

intact organism: a minimal model of insulin kinetics in the dog. *Diabetes*, 29:979–990, 1980.

[99] S. Welch, S. S. P. Gebhart, R. N. Bergman, and L. S. Phillips. Minimal model analysis of intravenous glucose tolerance test-derived insulin sensitivity in diabetic subjects. *J. Clin. Endocr. Metab.*, 71(6):1508–1518, 1990.

[100] X. J. Wen, Z. M. Wu, and J. G. Lu. Stability Analysis of a Class of Nonlinear Fractional–Order Systems. *IEEE T. Circuits. Syst. II, Exp. Briefs*, 55(11):1178–1182, 2008.

[101] S. Westerlund. Dead matter has memory! *Phys. Scripta.*, 43(2):174, 1991.

[102] Wikipedia. Diabetes mellitus— Wikipedia, the free encyclopedia. Online; accessed 20-May-2013.

[103] S. Wild, G. Roglic, A. Green, R. Sicree, and H. King. Global Prevalence of Diabetes: Estimates for the year 2000 and projections for 2030. *Diabetes Care*, 27(5):1047–1053, 2004.

국문초록

이 논문에서는 우리는 인슐린 민감성 (S_I) 과 포도당 효율성 (S_G) 을 잴 수 있는 주요한 글루코스–인슐린 역학 모델들을 소개하고 수학적인 분석을 통하여 그 모델들의 장단점을 살펴보았다. 그리고 효율적인 수치 알고리즘을 통해, 각 모델들에 대한 수치 해를 계한하였으며 그에 따른 변수민감도 분석도 진행하였다.

또한 인슐린 민감성을 측정하는 데 널리 쓰이고 있는 MINMOD Millennium 모델에, 글루코스–인슐린의 유동성을 반영할 수 있는 $\alpha \in (0, 1]$계 분수 미분의 개념을 도입하여 적용하였다. 이와 같이 제안된 모델은 수학적 분석을 통해서 해가 음이 아닌 유한한 값을 가지며 안정평형한 점들을 가짐을 보였다. 그리고 정상인과 제2형 당뇨병환자들에 관한 데이터를 기반으로 가중 비선형 최소자승법, Levenberg–Marquardt 알고리즘, 그리고 분수의 Adams방법들을 이용하여 최적의 변수들을 추정하였다. 이러한 수치적 결과로부터 제2형 당뇨병환자에게서 S_I가 정상인들에 비해 현격히 낮음을 확인 할 수 있었다. 또한 당내성을 결정하는 새로운 인자 ($\tau^{1-\alpha}$)의 확인과 그와 관련된 S_I의 관계를 밝혀냈다.

주요어: 글루코스–인슐린 역학, 인슐린 민감성, 미니멀모델, 분수미분

학번: 2010-30928

감사의 글

우선 하나님 아버지의 은총에 감사드립니다. 논문이 완성되기까지 부족한 저에게 충고와 관심을 아끼지 않으셨던 지도교수님이신 신동우 선생님께 감사드립니다. 바쁘신 와중에도 저의 박사학위논문의 심사를 맡아주신 정상권 선생님, 전영목 선생님, 박춘재 선생님께 감사드립니다. 그리고 심사위원이시고 여러가지로 저에게 많은 도움을 주신 임범누나에게도 정말 감사드립니다. 또한, 제 가족들, 외가 식구들, 친가 식구들, 우리 NASC랩 선후배들, 대학원 06학번 동기들, 예전 411B호 멤버들, 학부 친구들과 미처 언급되지 못 한 저를 아껴주시는 모든 분들께 감사드립니다. 앞으로 더욱 열심히 하도록 하겠습니다.